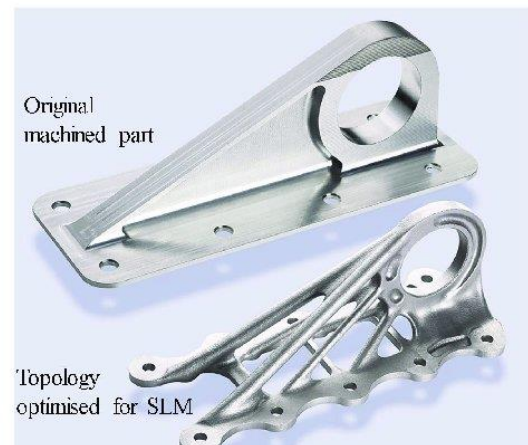
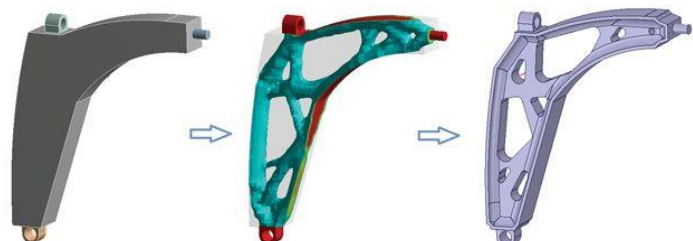




MAEG5160: Design for Additive Manufacturing

Lecture 24: Summary

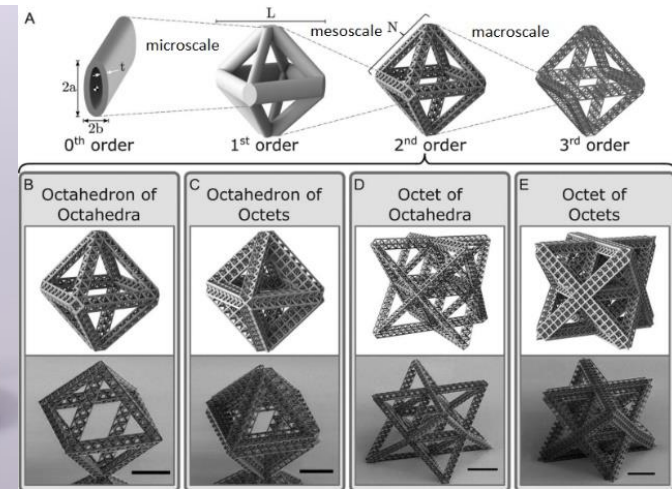


Prof SONG Xu

Department of Mechanical and Automation Engineering,
The Chinese University of Hong Kong.

Lecture 24: Summary

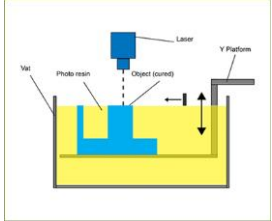
1. Topology optimization ✓
2. Multiscale structure design
3. Multi-material design
4. Design for mass customization
5. Parts consolidation ✓
6. Lattice structures ✓



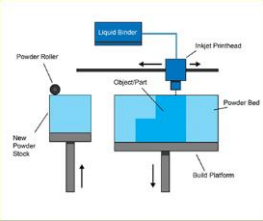
Lecture 24: Summary

Additive Manufacturing (AM)

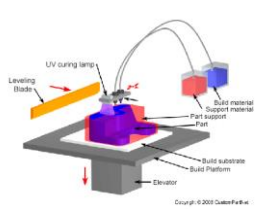
Vat Photopolymerization



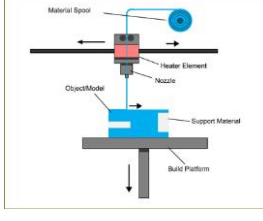
Binder Jetting



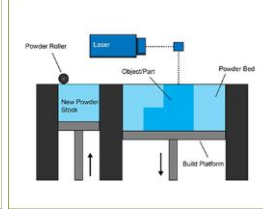
Material Jetting



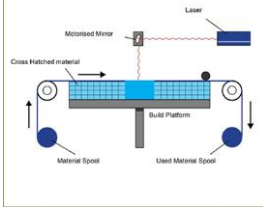
Material Extrusion



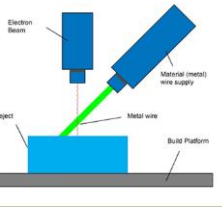
Powder Bed Fusion



Sheet Lamination

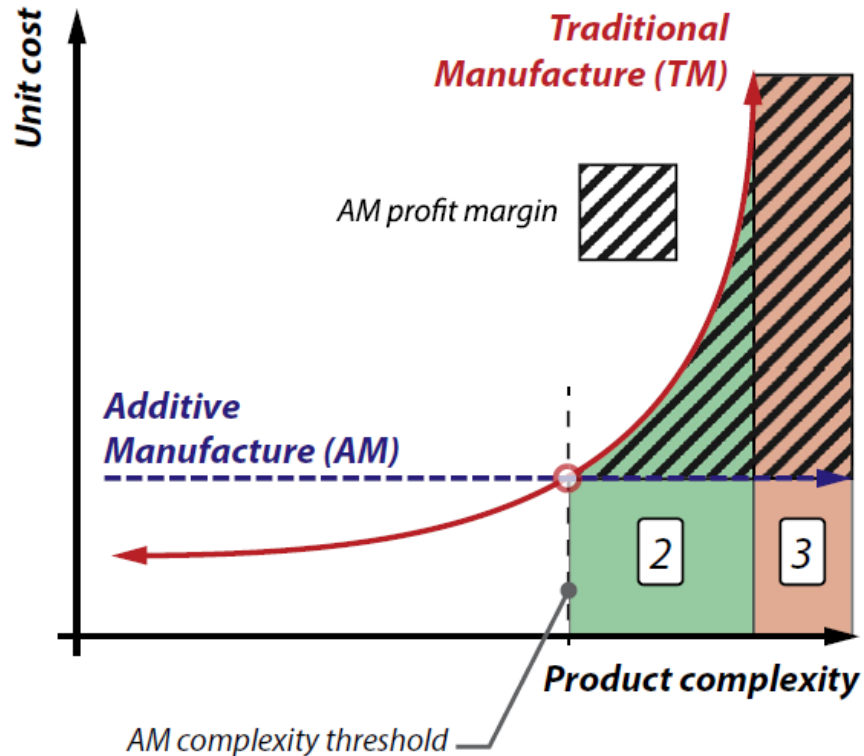
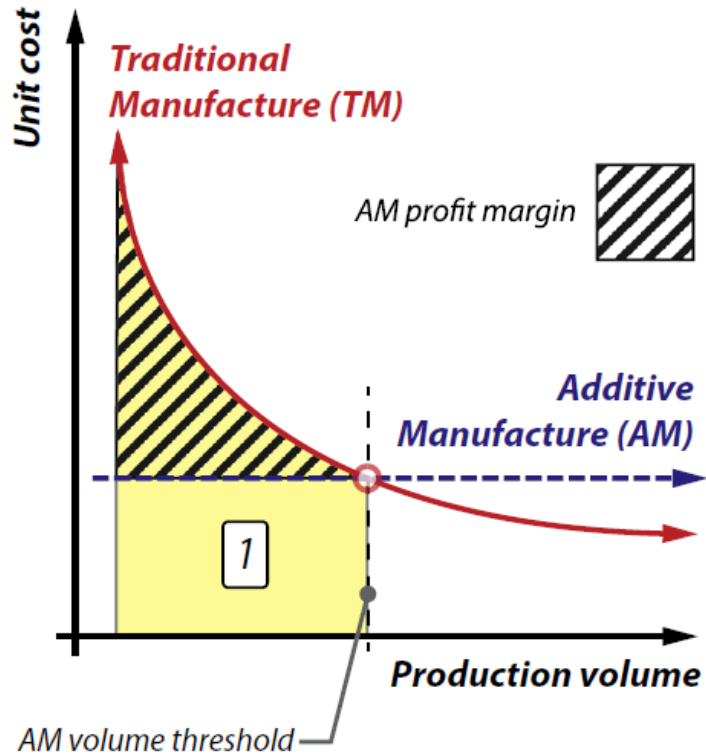


Directed Energy Deposition



Lecture 24: Summary

AM economically advantageous scenario



Zone 1: Batch-enabled scenarios.

Zone 2: Complexity-enabled scenarios.

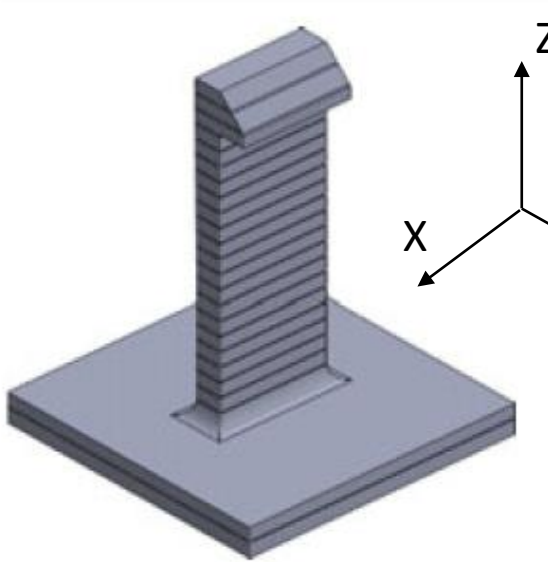
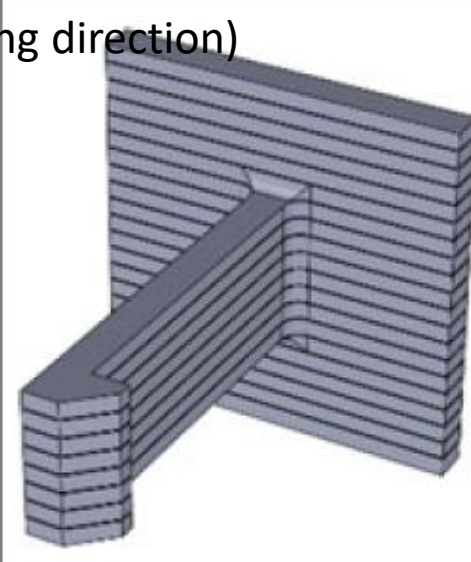
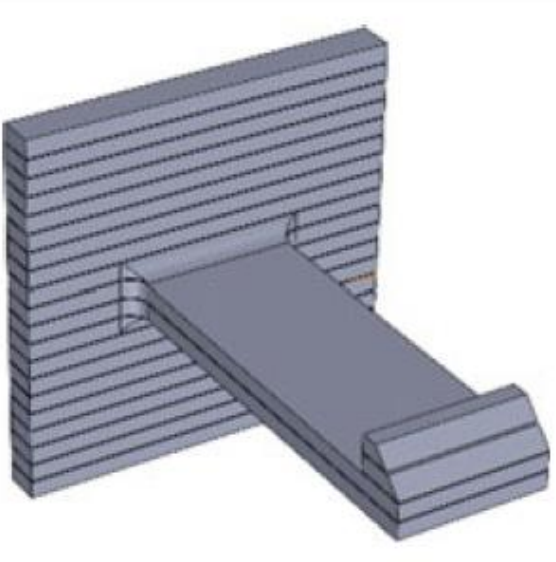
Zone 3: Ultra-high complexity scenarios.

Lecture 24: Summary

Design for polymer AM

Anisotropy

Implication/example

 Z (stacking direction)		
Clip will be weak and, almost certainly, break	Good compromise clip, with decent spring and strong hook	Clip has the best spring strength and flexibility but a weak hook

Lecture 24: Summary

Design for polymer AM

Wall thickness

In general, for light-weight consumer products, this ranges from around 0.6–2.5 mm, and for more industrial heavy-duty industrial products, this can range from 3 to 5 mm. Though it is possible to create thinner walls, how successfully they will print will depend on the surface area of the wall, and the unsupported width to height ratio.

Large surface area flat thin walls will be hard to print without distortion and, depending on the AM technology used, may delaminate. A simple technique to avoid this problem, if the wall cannot be made thicker, is using ribs to reinforce the wall. A general rule of thumb is to use even wall thicknesses throughout the parts, as uneven wall thicknesses can create part distortion.



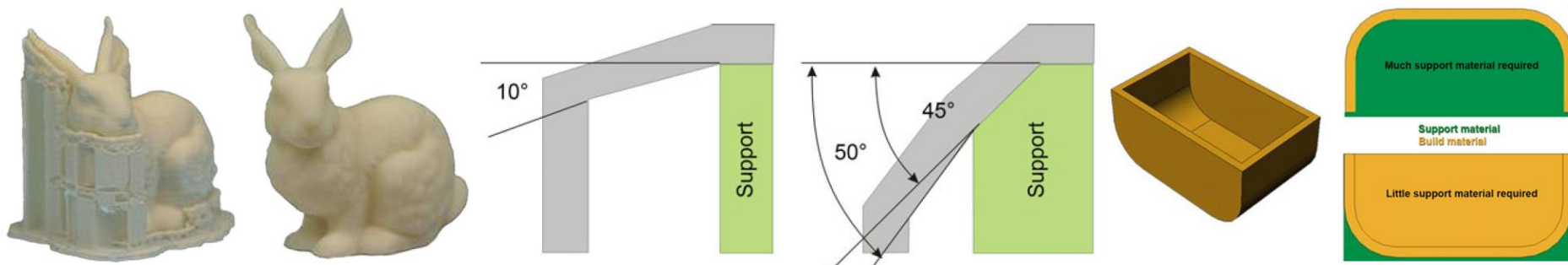
Lecture 24: Summary

Design for polymer AM

Overhangs and Support Material

Almost all polymer AM technologies, with the exception of powder bed fusion, and some binder jetting technologies, the printed parts require support material to support any overhanging features. Support material is a sacrificial material that is utilized during the printing process to allow any features that overhang, because it is not possible to print in air without the material collapsing, and is removed after the part has finished printing.

There is usually a support ‘angle’ option in your 3D printing software that determines the angle in which the part requires support material (a very rough starter is 45 degrees). Some printers measure this angle from the vertical, while others measure it from the horizontal. It is therefore important to be aware of how each particular printer takes this measurement.



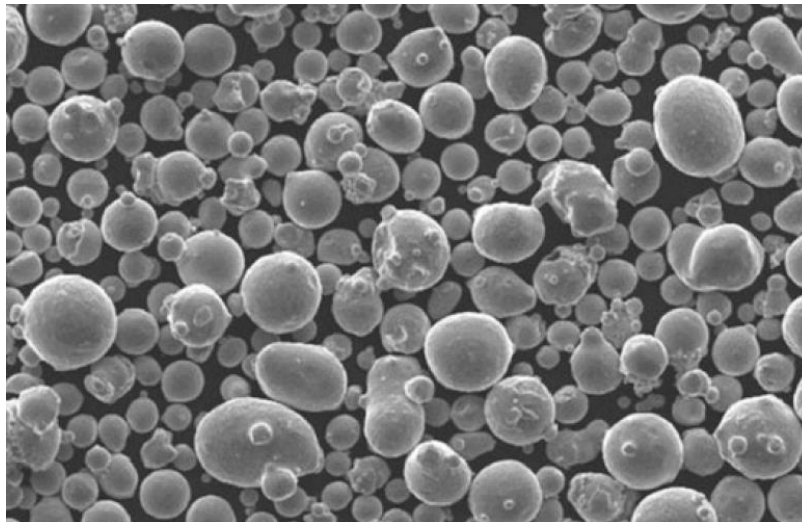
Lecture 24: Summary

Design for metal AM

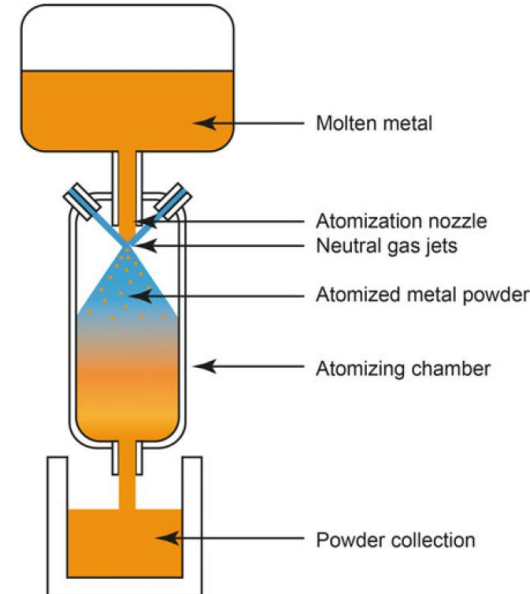
Metal Powder Production and Characteristics

Metal AM powder is, most commonly, made through a gas atomization process. There are a number of different atomisation processes including gas atomisation, vacuum induction melting gas atomisation, plasma atomisation, centrifugal atomisation, and water atomisation. Most of these atomization processes produce:

- A spherical powder shape
- A good powder density, thanks to the spherical shape and particle size distribution
- A good reproducibility of particle size distribution



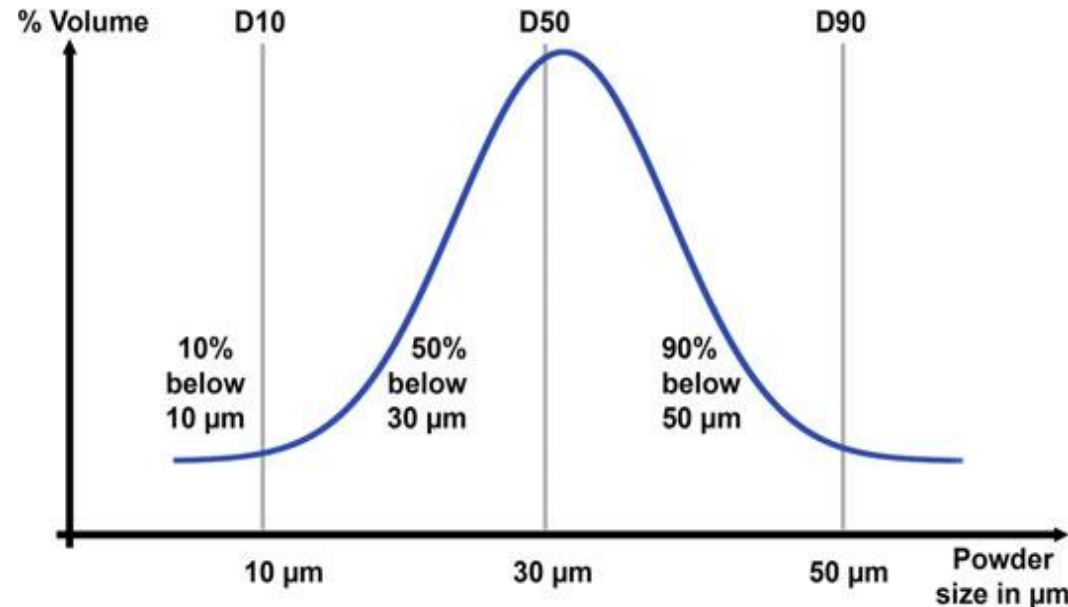
Gas atomisation process and resultant powder



Lecture 24: Summary

Design for metal AM

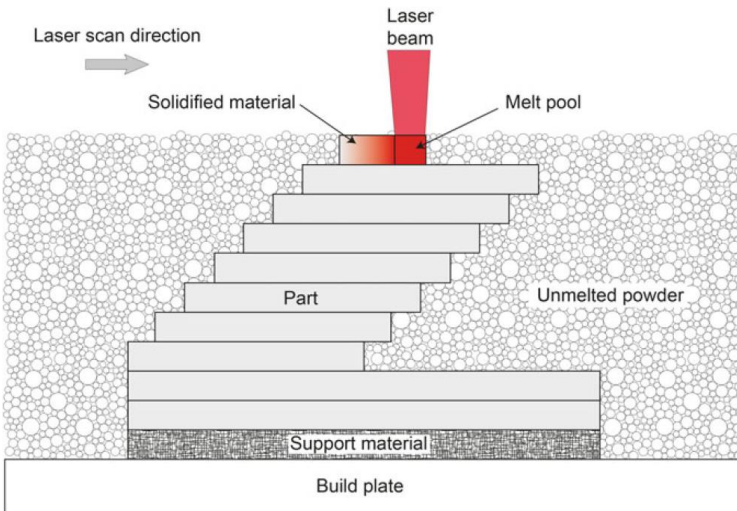
For powder-bed fusion the powder size most commonly used is between 30 and 40 μm , with a bell-curve distribution with some large and some smaller particles. Some systems that allow for very thin layer thicknesses may require smaller particle sizes. Some materials, such as aluminium, for example, may have a slightly larger powder size distribution than, say, steel or titanium. Larger powder sizes of between 50 and 100–150 μm are commonly used for EBM and DED technologies. The reason a mixed powder size distribution is desirable is so that the smaller particles fit between the larger ones, and allow a denser layer of powder to be spread. If all the particles are exactly of the same size, this will leave gaps between the spread powder particles, which will cause it to collapse, or shrink, more during the melting process.



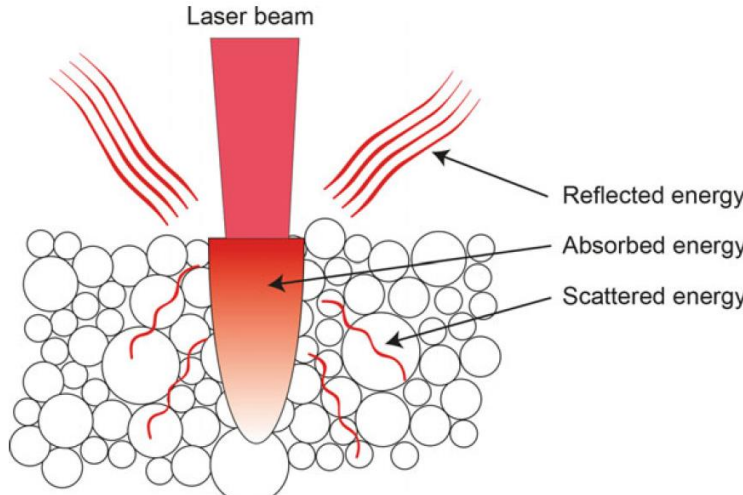
Lecture 24: Summary

Design for metal AM

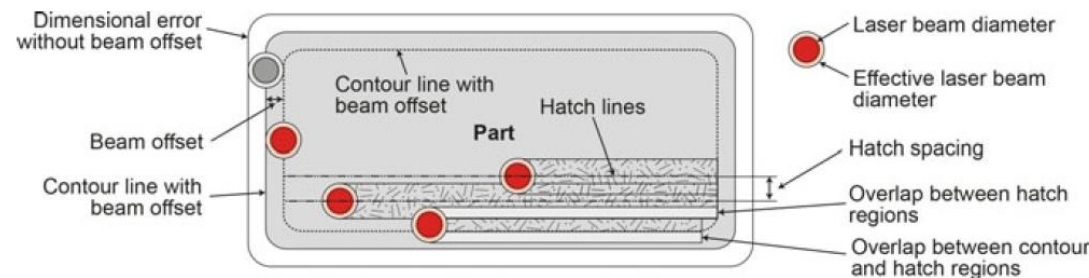
Powder bed metal AM process



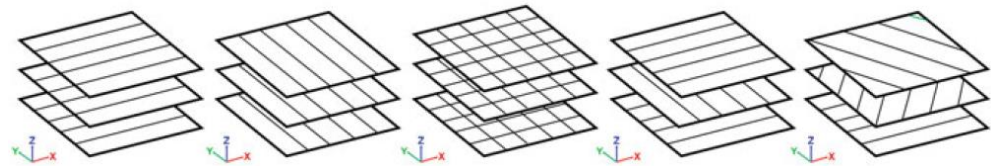
Overall powder bed metal AM build process



Effect of powder on energy beam absorption



Cross section details



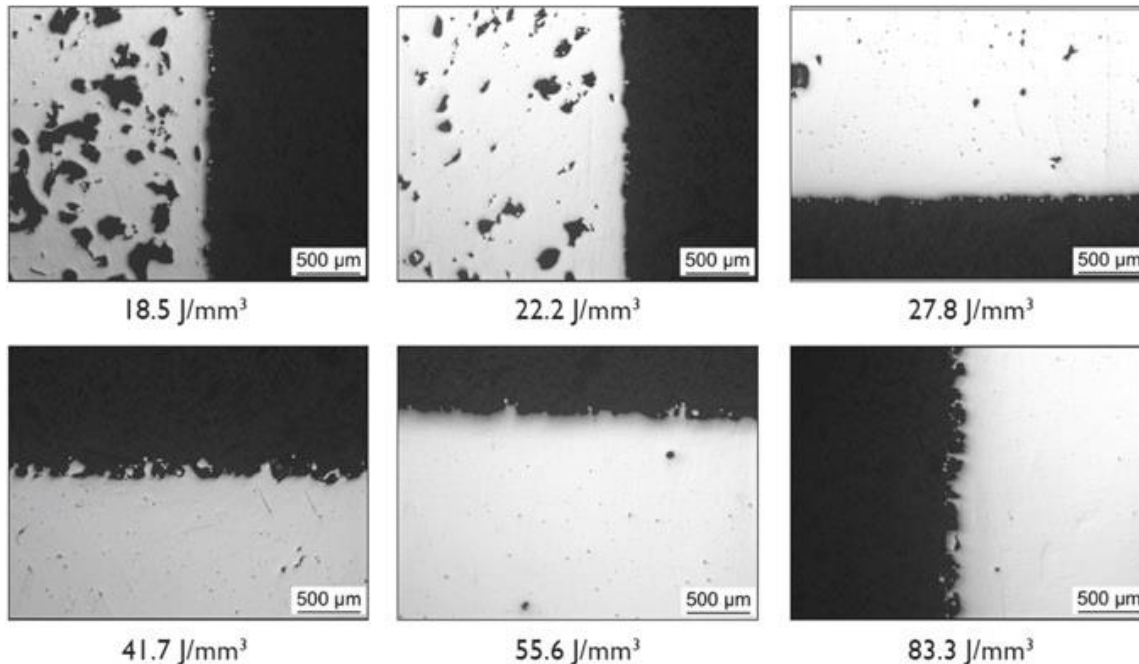
Different energy beam scanning strategy

There are also various scanning strategies that can be used in order to minimize the stress in each layer of the part so as to minimize part distortion. A common scanning strategy, for example, is to rotate the scan pattern for each successive layer by 67°. This avoids consecutive layers having exactly overlapping scan patterns, which could increase residual stress in the part.

Lecture 24: Summary

Design for metal AM

Powder bed metal AM process – energy density



E = energy density

P = Power (W)

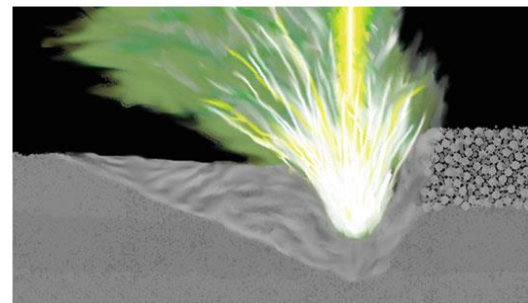
$$E = \frac{P}{v \cdot h \cdot t}$$

v = Scanning speed (mm/s)

h = hatch spacing (mm)

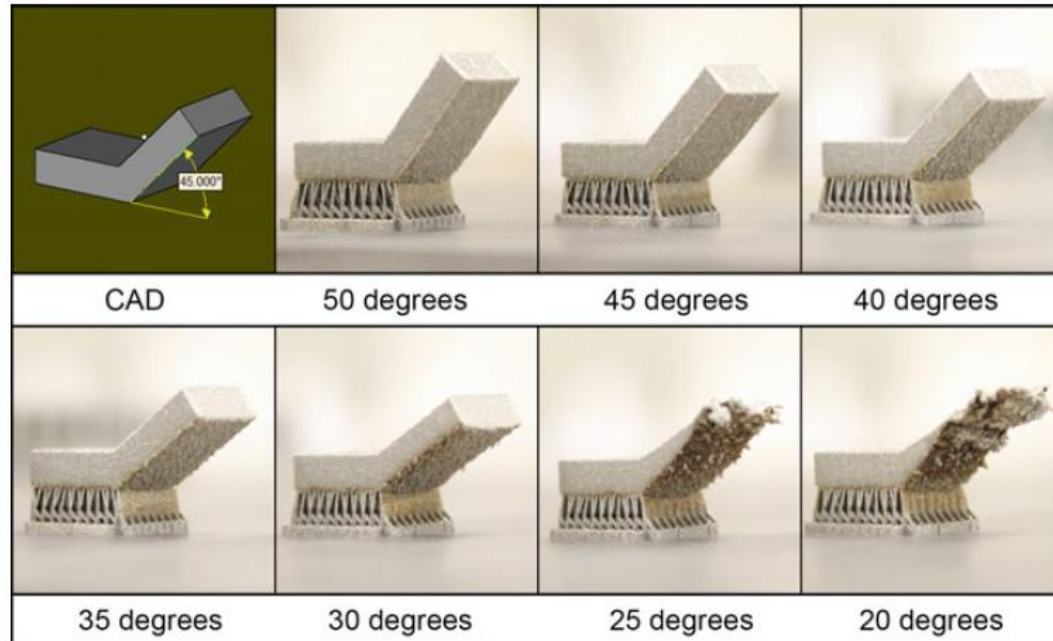
t = layer thickness (mm)

In the example below, using Ti6Al4 V as the material, energy densities above 40 J/mm³ are needed to obtain parts with 99.7–99.9% relative density. As the energy density increases beyond that, part density continues to improve but surface roughness gets worse. This is because the increased energy causes the molten material to be violently agitated, which results in a rougher surface. At an energy density of 30 J/mm³, however, the part is slightly less dense (but generally still better than 99% dense) but the part has both improved surface quality and minimized defects at the borders.

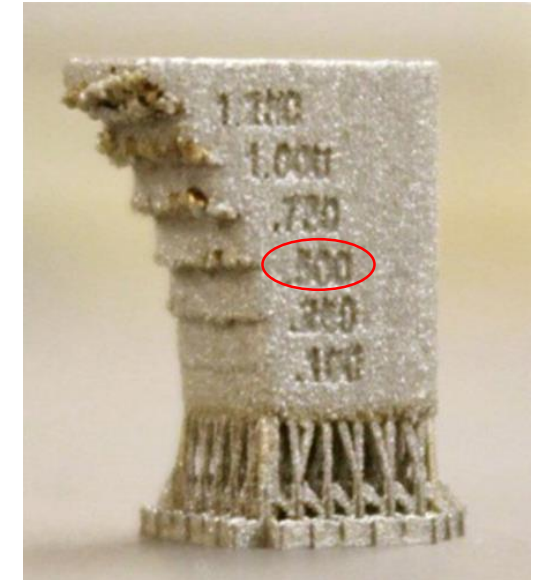


Lecture 24: Summary

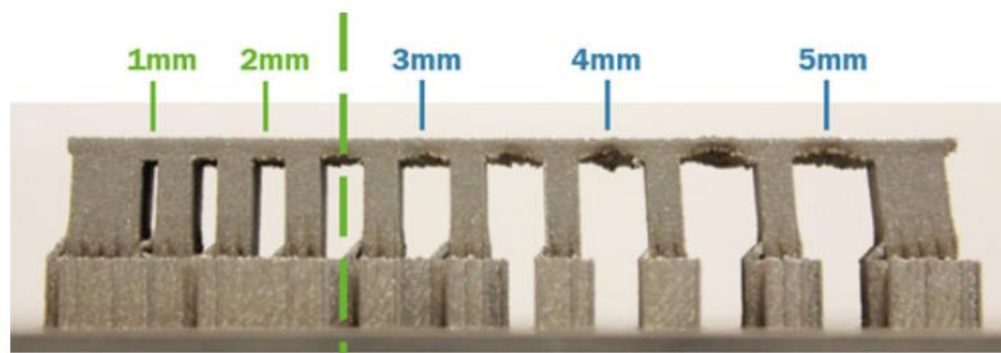
Design for metal AM



A general rule of thumb for angles that do not require support material are angles greater than 45° from horizontal.



In general, any design with an overhang greater than 0.5 mm will require additional support to prevent damage to the part.



The maximum allowable unsupported distance for the powder bed fusion process is around 2 mm.

Lecture 24: Summary

Design for metal AM

If large masses of material are completely unavoidable (which is rare), use different laser hatch parameter settings to minimize the build-up of residual stress.

- Smaller chess-board hatch patterns will, for example, create less residual stress than bigger ones, or than large scan areas. But they will slow down the build process a bit.
- Rotate each hatch scan, usually by 67° , for each layer.



Meander hatch pattern

High build rate

Higher residual stress

Suitable for small/thin parts

Stripe hatch pattern

Medium build rate

Medium residual stress

Suitable for large parts

Chessboard hatch pattern

Slow build rate

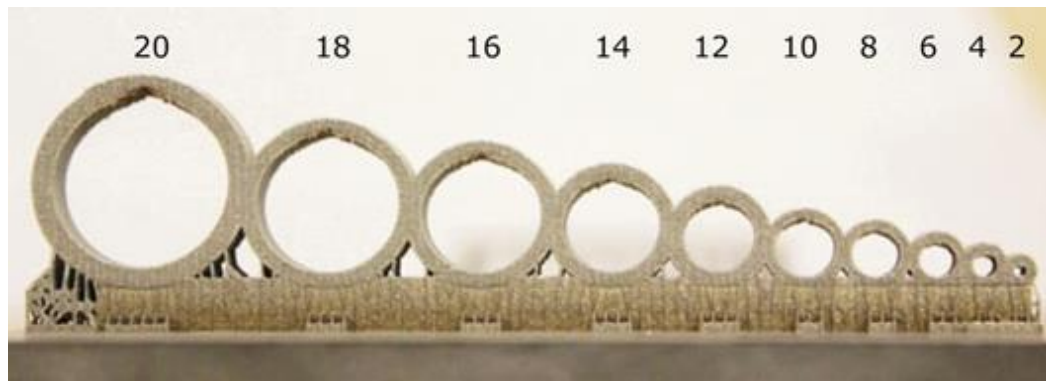
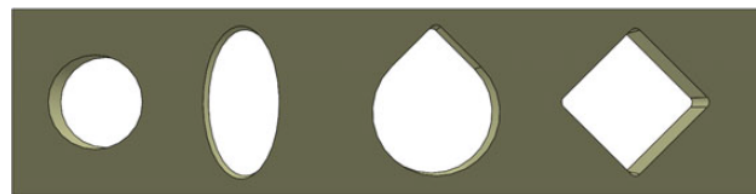
Lower residual stress

Suitable for large parts

Lecture 24: Summary

Horizontal Holes

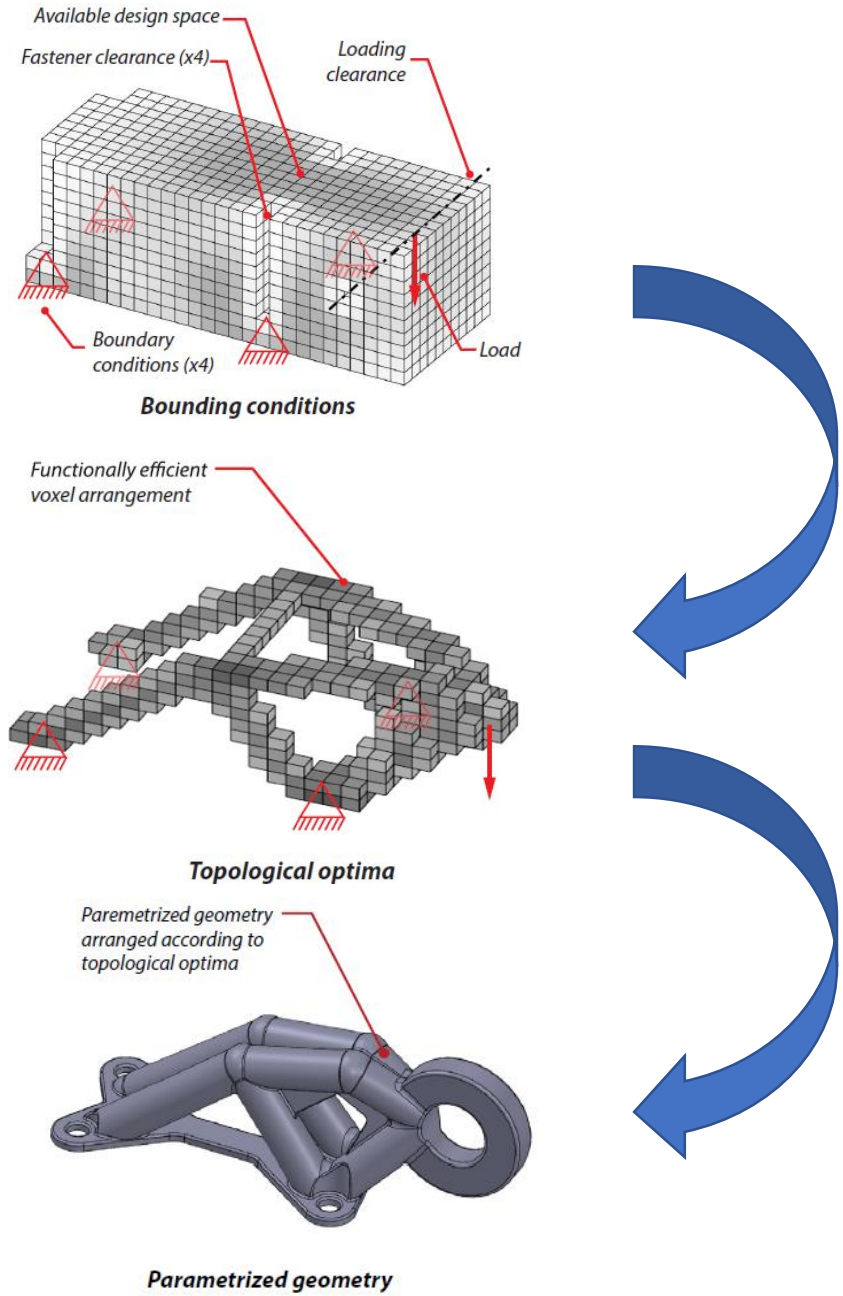
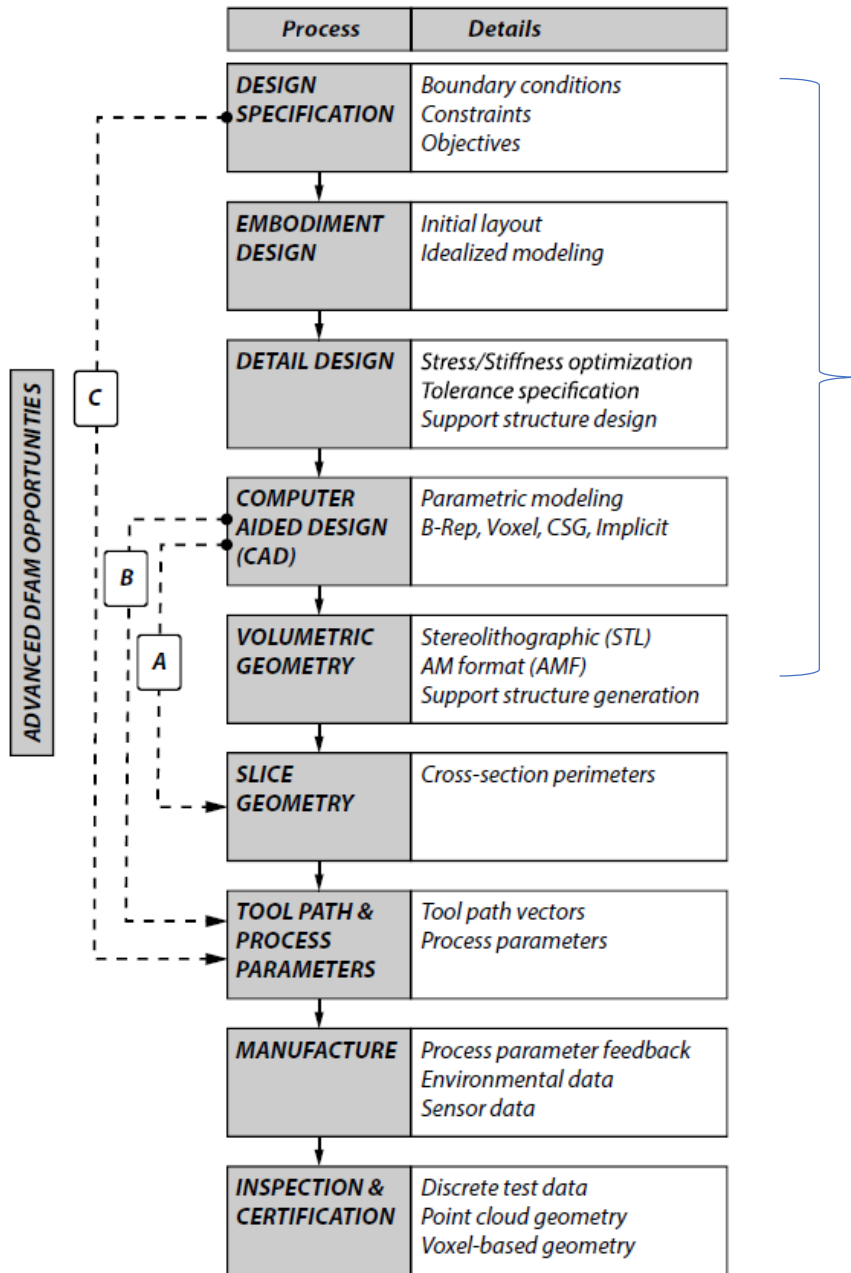
In metal AM, horizontal holes (or holes angled below the minimum support angle) over a certain diameter will require support material inside the hole. Though this is not necessarily a problem, it should be remembered that it is always harder to remove support material from inside the part than from outside the part. For long holes or pipes that are not perfectly straight, in particular, the support can be hard to remove from inside the pipe. As a general guideline, holes below a diameter of 8 mm can be printed without supports. If larger holes are required, the most common technique is to change the hole from a circular to a shape that can be printed without the need for support material. These shapes commonly include ellipses, teardrops, and diamonds.



Round holes can, generally, be built without support up to a diameter of around 8mm. Holes larger than this will require supports. Note that this diameter varies based on the machine and material used.	Elliptical holes, when the height of the ellipse is twice the width, can be printed to about 25mm tall, depending on the system being used.	Teardrop shaped holes can be printed to almost any diameter providing the top angle is no less than the minimum support angle. It is good practice to fillet the top of the teardrop to avoid a stress concentration.	Diamond shaped holes can be printed to almost any size. It is good practice to fillet the corners of the hole to avoid stress concentrations in the corners.
---	---	---	--

Lecture 24: Summary

Digital design for AM



Basic concept of digital design and design optimization: design can be numerated, and compared numerically.

Selecting the “best” design within the available means

1. What is our criterion for “best” design? Objective function
 2. What are the available means? Constraints
(design requirements)
 3. How do we describe different designs? Design Variables

Lecture 24: Summary

Optimization statement

Minimize $f(\mathbf{x})$

Subject to $g(\mathbf{x}) \leq 0$

$h(\mathbf{x}) = 0$

$f(\mathbf{x})$: Objective function to be minimized

$g(\mathbf{x})$: Inequality constraints

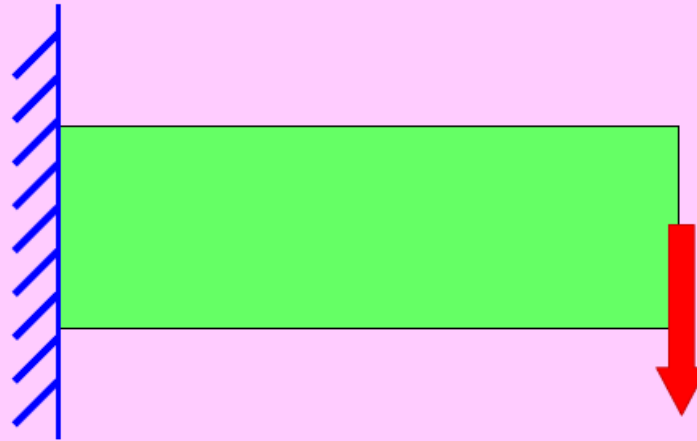
$h(\mathbf{x})$: Equality constraints

\mathbf{x} : Design variables

Lecture 24: Summary

Design Optimization

minimize $f(\mathbf{x})$
subject to $g(\mathbf{x}) \leq 0$
 $h(\mathbf{x}) = 0$



BC's are given

Loads are given

1. To make the structure strong
e.g. Minimize displacement at the tip

→ *Min. $f(\mathbf{x})$*

2. Total mass $\leq M_c$

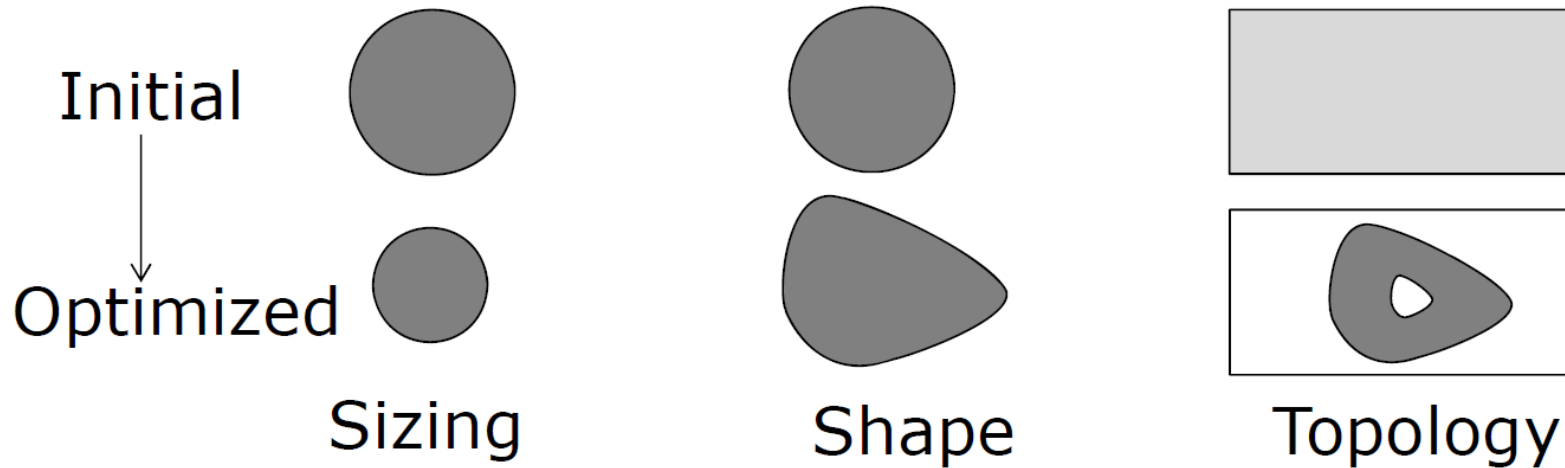
→ *$g(\mathbf{x}) \leq 0$*

Lecture 24: Summary

Design Optimization

Selecting the best “structural” design

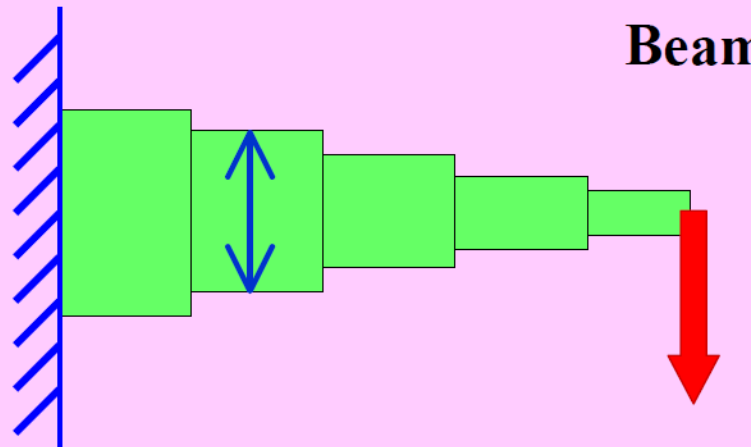
- Size Optimization
- Shape Optimization
- Topology Optimization



Lecture 24: Summary

Size Optimization

minimize $f(\mathbf{x})$
subject to $g(\mathbf{x}) \leq 0$
 $h(\mathbf{x}) = 0$



Beams

Design variables (\mathbf{x})

\mathbf{x} : thickness of each beam

$f(\mathbf{x})$: compliance

$g(\mathbf{x})$: mass

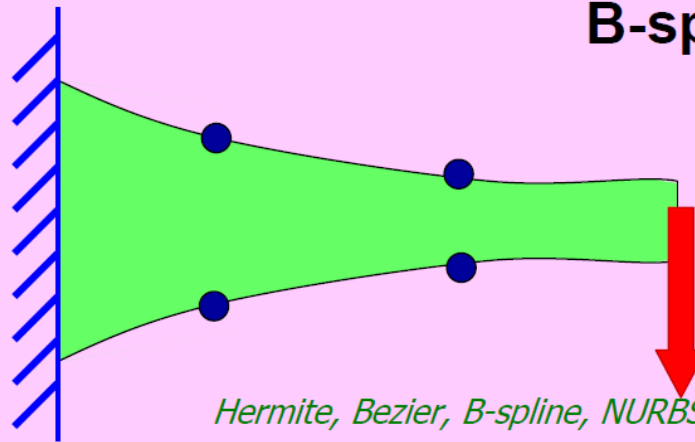
Number of design variables (ndv)

ndv = 5

Lecture 24: Summary

Shape Optimization

minimize $f(\mathbf{x})$
subject to $g(\mathbf{x}) \leq 0$
 $h(\mathbf{x}) = 0$



Design variables (\mathbf{x})

\mathbf{x} : control points of the B-spline
(position of each control point)

$f(\mathbf{x})$: compliance

$g(\mathbf{x})$: mass

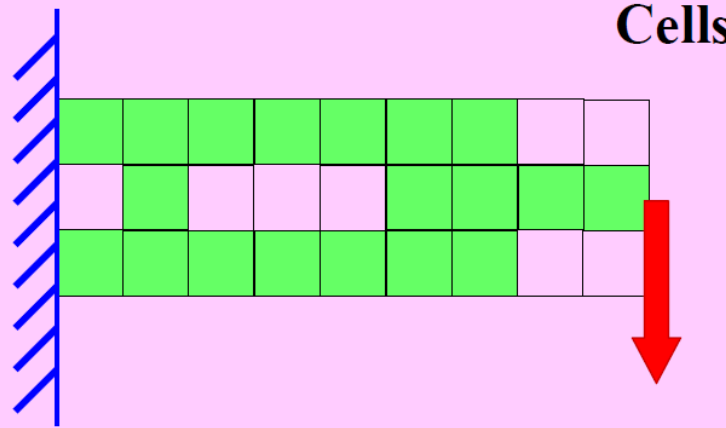
Number of design variables (ndv)

$ndv = 8$

Lecture 24: Summary

Topology Optimization

minimize $f(\mathbf{x})$
subject to $g(\mathbf{x}) \leq 0$
 $h(\mathbf{x}) = 0$



Design variables (\mathbf{x})

\mathbf{x} : density of each cell

Number of design variables (ndv)

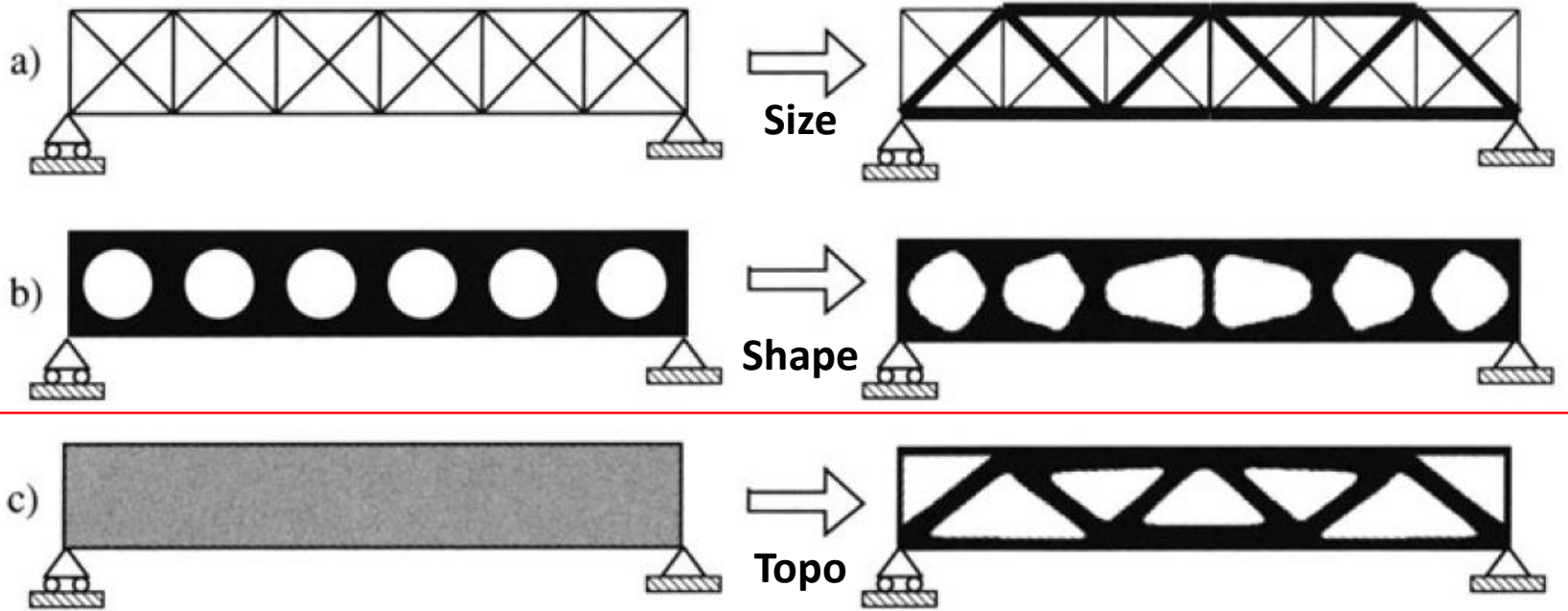
$ndv = 27$

$f(\mathbf{x})$: compliance

$g(\mathbf{x})$: mass

Lecture 24: Summary

Recall: Three types of design optimization: size, shape and topology



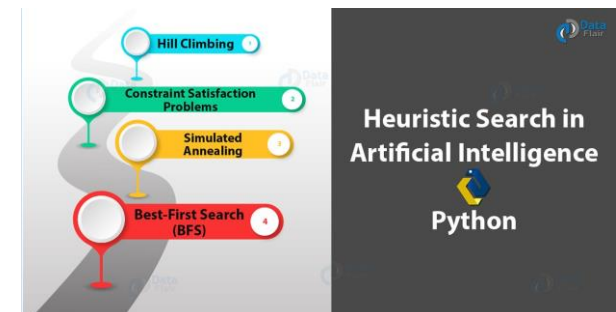
Lecture 24: Summary

Optimization method: Gradient-based method

Steepest Descent	UNCONSTRAINED
Conjugate Gradient	
Quasi-Newton	
Newton	
Simplex – linear	CONSTRAINED
SLP – linear	
SQP – nonlinear, expensive, common in engineering applications	
Exterior Penalty – nonlinear, discontinuous design spaces	
Interior Penalty – nonlinear	
Generalized Reduced Gradient – nonlinear	
Method of Feasible Directions – nonlinear	
Mixed Integer Programming	

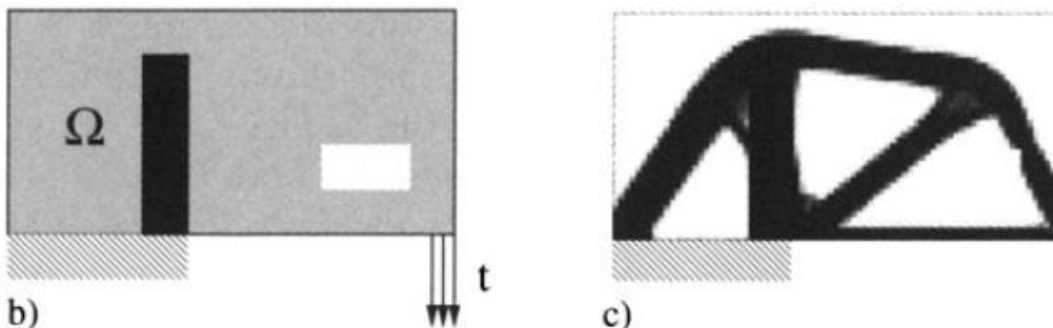
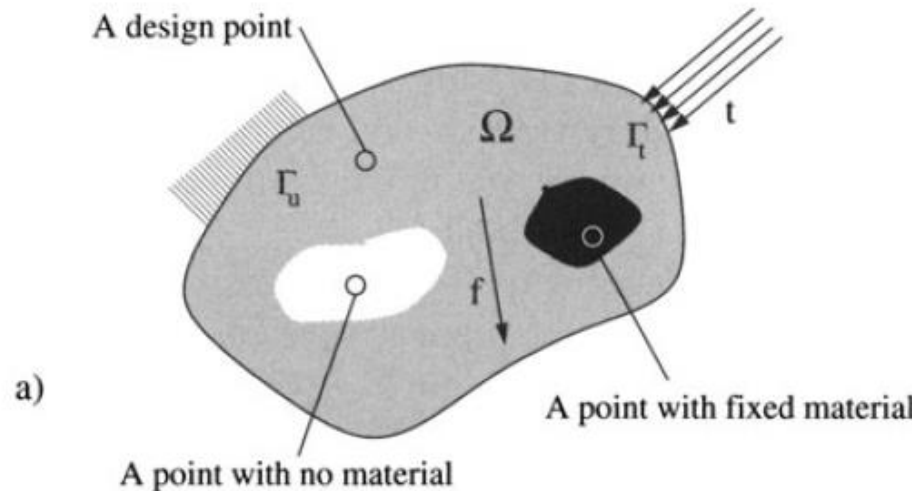
Optimization method: Heuristic method

- Heuristics Often Incorporate Randomization
- **3 Most Common Heuristic Techniques**
 - Genetic Algorithms
 - Simulated Annealing
 - Tabu Search



Lecture 24: Summary

Topology Optimization (TO) by distribution of isotropic material



The generalized topology design problem of finding the optimal material distribution in a two-dimensional domain

Lecture 24: Summary

Introducing the energy bilinear form (i.e., the internal virtual work of an elastic body at the equilibrium u and for an arbitrary virtual displacement v)

$$a(u, v) = \int_{\Omega} E_{ijkl}(x) \varepsilon_{ij}(u) \varepsilon_{kl}(v) d\Omega$$

with linearized strains $\varepsilon_{ij}(u) = \frac{1}{2} \left(\frac{\partial u_i}{\partial x_j} + \frac{\partial u_j}{\partial x_i} \right)$ and the load energy linear form

$$l(u) = \int_{\Omega} f u d\Omega + \int_{\Gamma_T} t u ds$$

the minimum compliance (maximum global stiffness) problem takes the form

$$\begin{aligned} & \min_{u \in U, E} l(u) \\ \text{s.t. : } & a_E(u, v) = l(v), \quad \text{for all } v \in U \\ & E \in \mathbf{E}_{\text{ad}} . \end{aligned}$$

Lecture 24: Summary

Discretize the problem using finite elements. It is here important to note that there are *two* fields of interest, namely both the displacement u and the stiffness E . If we use the same finite element mesh for both fields, and discretize E as constant in each element,

$$\begin{aligned} & \min_{\mathbf{u}, E_e} \mathbf{f}^T \mathbf{u} \\ \text{s.t. : } & \mathbf{K}(E_e) \mathbf{u} = \mathbf{f}, \\ & E_e \in \mathbb{E}_{\text{ad}} . \end{aligned}$$

Here \mathbf{u} and \mathbf{f} are the displacement and load vectors, respectively. The stiffness matrix \mathbf{K} depends on the stiffness E_e in element e , numbered as $e = 1, \dots, N$, and we can write \mathbf{K} in the form

$$\mathbf{K} = \sum_{e=1}^N \mathbf{K}_e(E_e)$$

Lecture 24: Summary

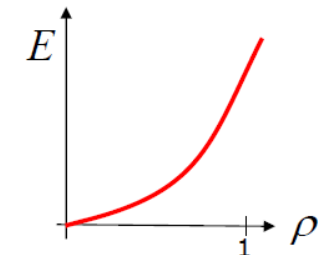
The most commonly used approach to solve this problem is to replace the integer variables with continuous variables and then introduce some form of penalty that steers the solution to discrete 0-1 values. The design problem for the fixed domain is then formulated as a sizing problem by modifying the stiffness matrix so that it depends continuously on a function which is interpreted as a density of material. This function is then the design variable. The requirement is that the optimization results in designs consisting almost entirely of regions of material or no material. This means that intermediate values of this artificial density function should be penalized in a manner analogous to other continuous optimization approximations of 0-1 problems. One possibility which has proven very popular and extremely efficient is the so-called penalized, proportional stiffness model (the SIMP-model)

$$E_{ijkl}(x) = \rho(x)^p E_{ijkl}^0, \quad p > 1,$$

$$\int_{\Omega} \rho(x) d\Omega \leq V; \quad 0 \leq \rho(x) \leq 1, \quad x \in \Omega$$

$$E_{ijkl}(\rho = 0) = 0, \quad E_{ijkl}(\rho = 1) = E_{ijkl}^0$$

Stiffness interpolation:



$$E(\rho_e) = E_1 + \rho_e^p (E_2 - E_1)$$

$$p > 1$$

by specifying a value of ρ higher than one makes it "uneconomical" to have intermediate densities in the optimal design. Thus the penalization is achieved without the use of any explicit penalization scheme. For problems where the volume constraint is active, experience shows that optimization does actually result in such designs if one chooses p sufficiently big (in order to obtain true "0-1" designs, $p > 3$ is usually required)

Lecture 24: Summary

Optimization:

Compute the optimal distribution over the reference domain of the design variable ρ . The optimization uses a displacement based finite element analysis and the optimality update criteria scheme for the density. The structure of the algorithm is:

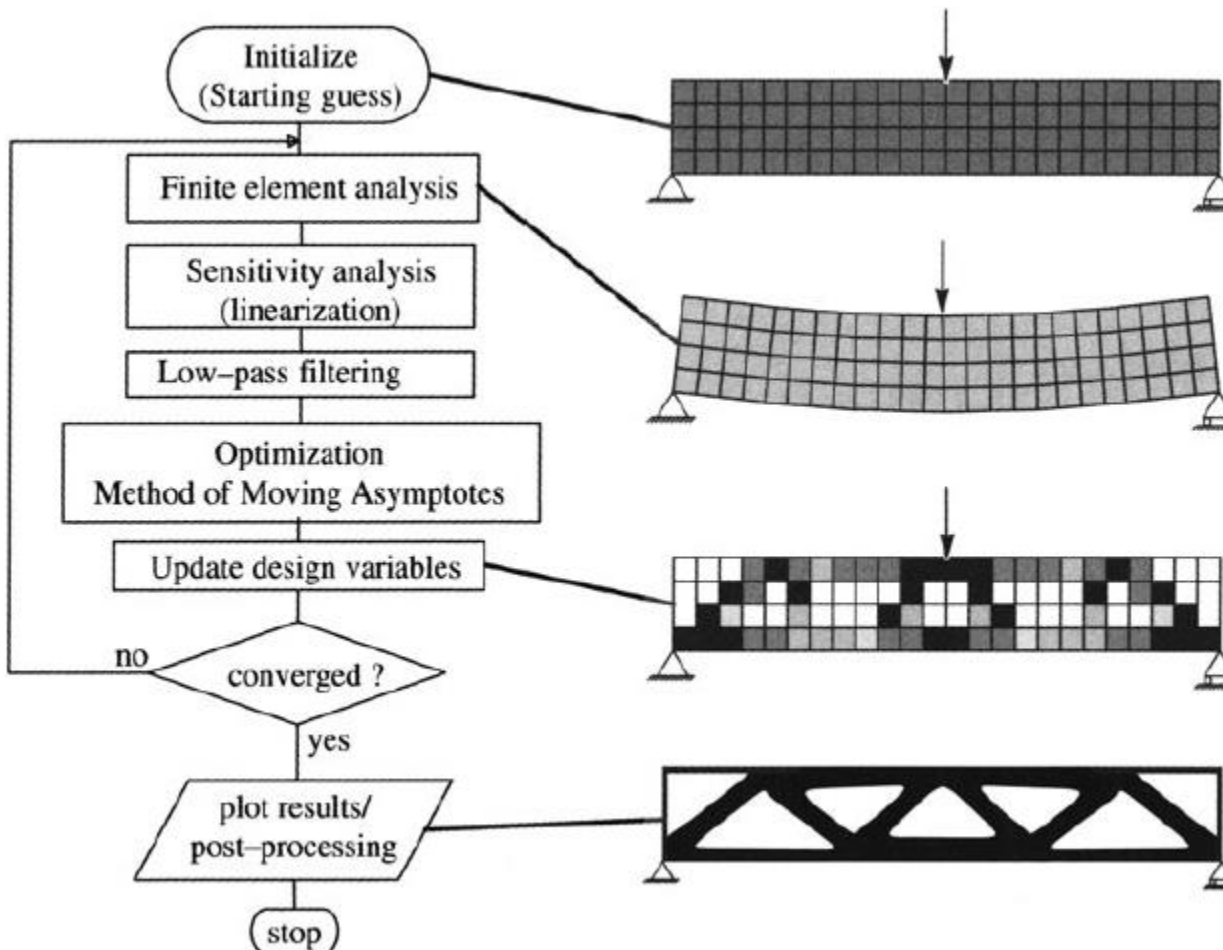
- Make initial design, e.g., homogeneous distribution of material. The iterative part of the algorithm is then:
- For this distribution of density, compute by the finite element method the resulting displacements and strains.
- Compute the compliance of this design. If only marginal improvement (in compliance) over last design, stop the iterations. Else, continue. For detailed studies, stop when necessary conditions of optimality are satisfied.
- Compute the update of the density variable, based on the scheme shown in section 1.2.1. This step also consists of an inner iteration loop for finding the value of the Lagrange multiplier Λ for the volume constraint.
- Repeat the iteration loop.

For a case where there are parts of the structure which are fixed (as solid and/or void) the updating of the design variables should only be invoked for the areas of the ground structure which are being redesigned (reinforced).

Post-processing of results:

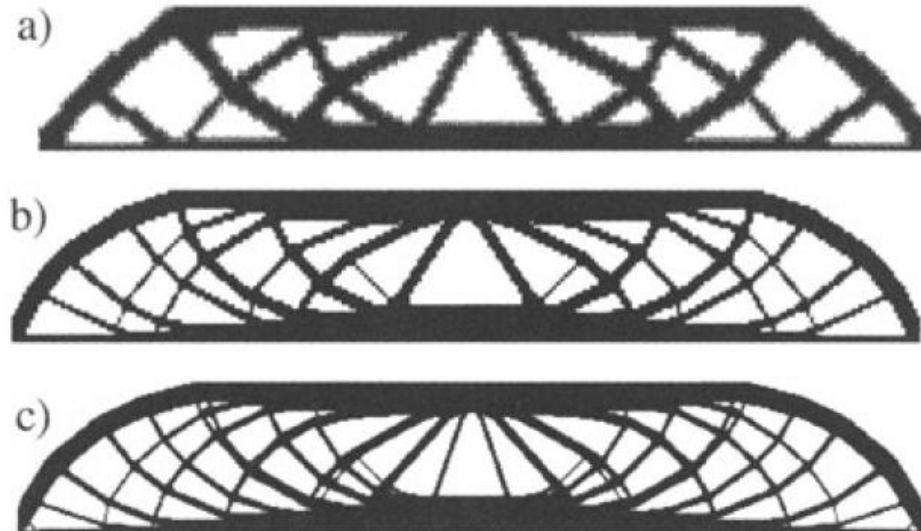
- Interpret the optimal distribution of material as defining a shape, for example in the sense of a CAD representation.

Lecture 24: Summary



Lecture 24: Summary

In the following we will discuss two important issues that significantly influences the computational results that can be obtained with the material distribution based topology design procedure. These are (1) *the appearance of checkerboards* and (2) *the mesh-dependency of results*. The former refers to the formation of regions of alternating solid and void elements ordered in a checkerboard like fashion and is related to the discretization of the original continuous problem. Mesh-dependence concerns the effect that qualitatively different optimal solutions are reached for different mesh-sizes or discretization and this problem is rooted in the issue of existence of solutions to the continuous problem.

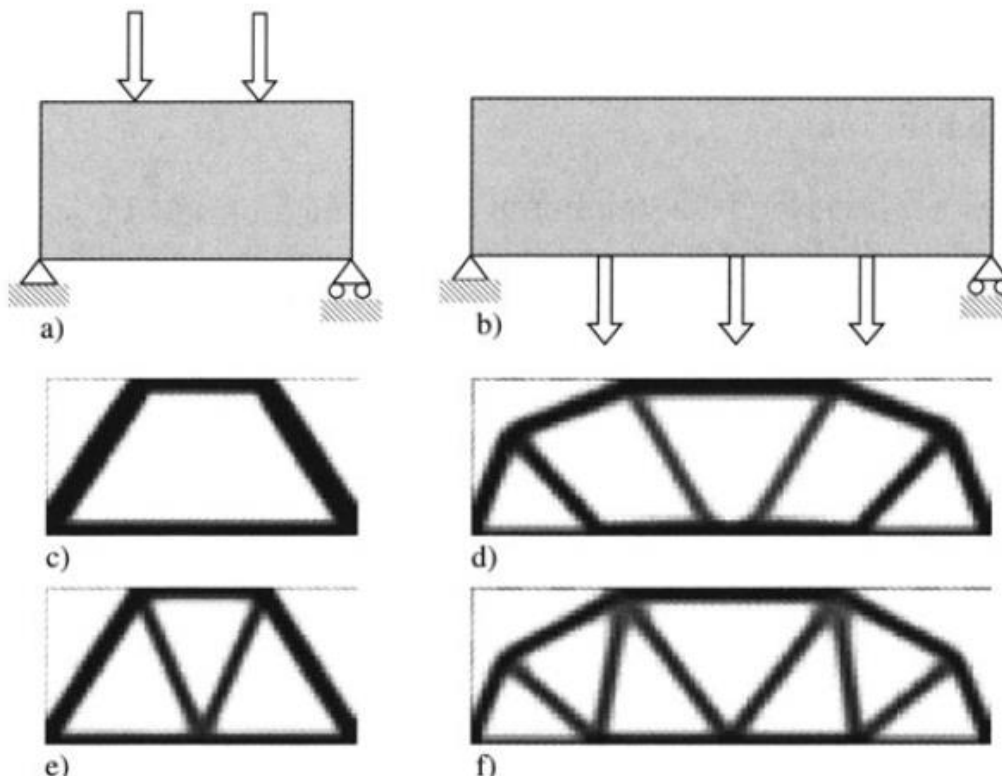


Dependence of the optimal topology on mesh refinement for the MBB beam example. Solution for a discretization with a) 2700, c) 4800 and d) 17200 elements.

Lecture 24: Summary

Variations of the conditions

Multiple loads



Example of differences in using one or more load cases. a) and b) Design domains. c) and d) Optimized topologies for all loads in one load case. e) and f) Optimized topologies for multiple loading cases. It is seen that single load problems result in unstable structures based on square frames whereas multi load case problems results in stable structures based on triangular frames.

Lecture 24: Summary

Extensions and applications:

1 Problems in dynamics

1.1 Free vibrations and eigenvalue problems

1.2 Forced vibrations

2 Buckling problems

3 Stress constraints

3.1 A stress criterion for the SIMP model

3.2 Solution aspects

4 Pressure loads

5 Geometrically non-linear problems

5.1 Problem formulation and objective functions

5.2 Choice of objective function for stiffness optimization

5.3 Numerical problems and ways to resolve them

5.4 Examples

6 Synthesis of compliant mechanisms

6.1 Problem setting

2.6.2 Output control

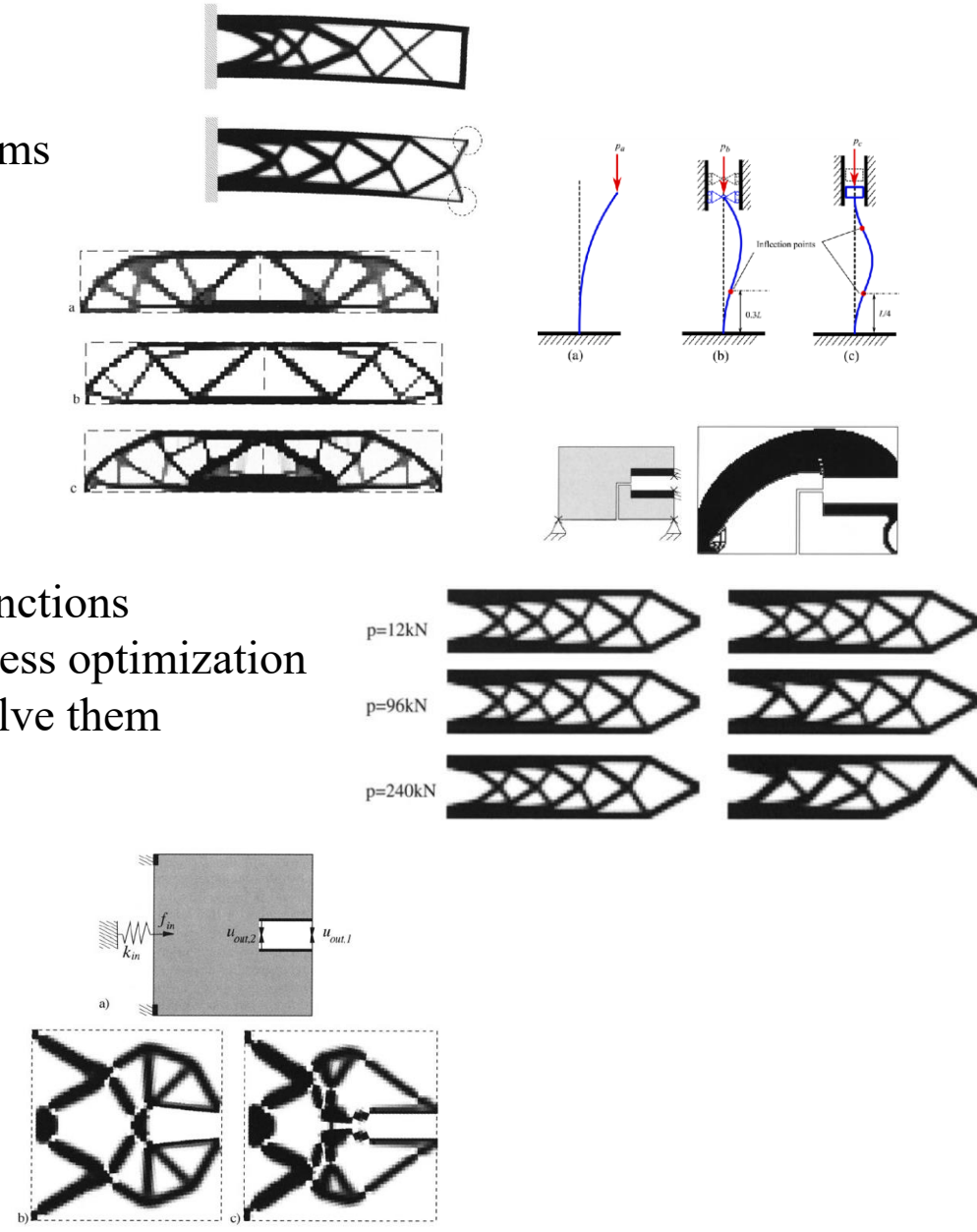
6.3 Path generating mechanisms

6.4 Linear modelling

6.5 Linear vs. non-linear modelling

6.6 Design of thermal actuators

6.7 Computational issues



Lecture 24: Summary

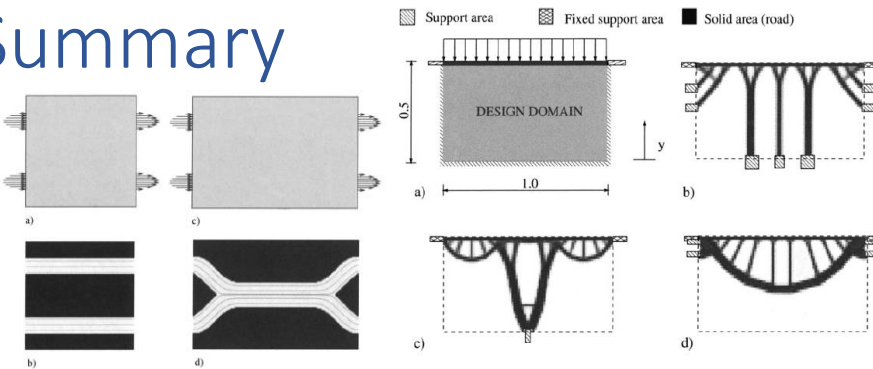
7 Design of supports

8 Alternative physics problems

8.1 Multiphysics problems

8.2 MicroElectroMechanical Systems (MEMS)

8.3 Stokes flow problems



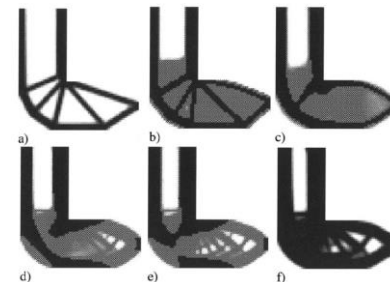
9 Optimal distribution of multiple material phases

9.1 One material structures

9.2 Two material structures without void

9.3 Two material structures with void

9.4 Examples of multiphase design

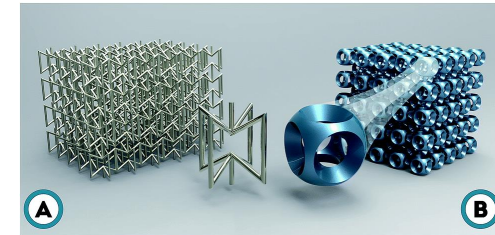


10 Material design

10.1 Numerical homogenization and sensitivity analysis

10.2 Objective functions for material design

10.3 Material design results

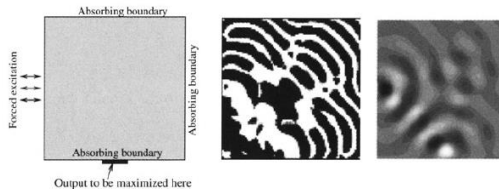


11 Wave propagation problems

11.1 Modelling of wave propagation

11.2 Optimization of band gap materials

11.3 Optimization of band gap structures



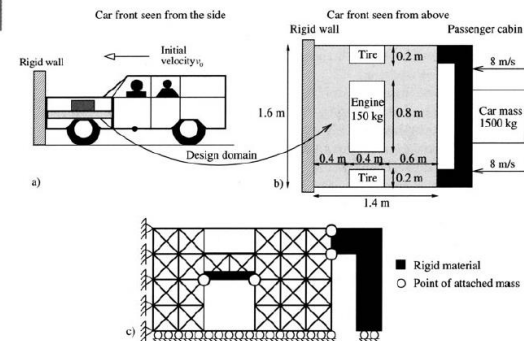
12 Various other applications

12.1 Material design for maximum buckling load

12.2 Crashworthiness

12.3 Bio-mechanical simulations

12.4 Applications in the automotive industry



Lecture 24: Summary

Application: Free vibrations and eigenvalue problem

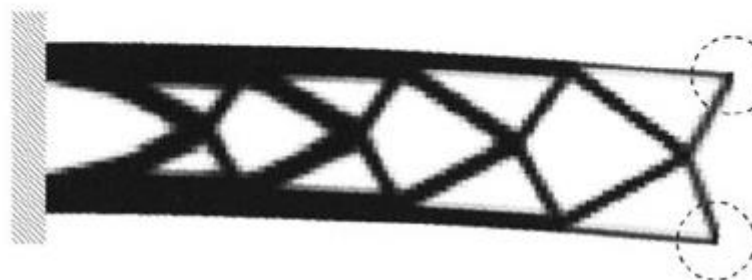
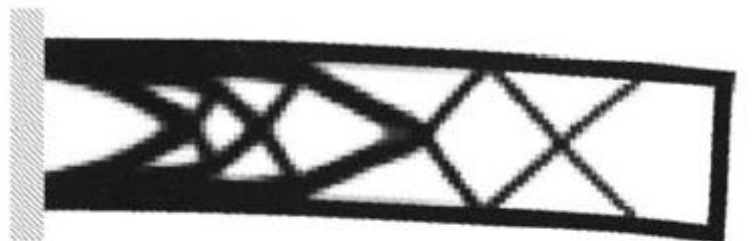
A commonly used design goal for dynamically loaded structures is the maximization of the fundamental eigenvalue λ_{min}

$$\begin{aligned} \max_{\rho} \quad & \left\{ \lambda_{min} = \min_{i=1, \dots, N_{dof}} \lambda_i \right\} \\ \text{s.t. : } & (\mathbf{K} - \lambda_i \mathbf{M}) \Phi_i = \mathbf{0}, \quad i = 1, \dots, N_{dof}, \\ & \sum_{e=1}^N v_e \rho_e \leq V, \quad 0 < \rho_{min} \leq \rho_e \leq 1, \quad e = 1, \dots, N, \end{aligned}$$

where \mathbf{K} and \mathbf{M} are the system stiffness and mass matrices, respectively and Φ_i is the eigenvector associated with the i 'th eigenvalue. In practice one does not solve for all N_{dof} modes of the eigenvalue problem. Only the first up to 10 modes will usually play a role in determining the dynamical response of a structure.

Note that the problem *as stated* has a trivial solution: one can in principle obtain an infinite eigenvalue by removing the entire structure. Therefore, the eigenvalue problem is often used in "reinforcement" problems where parts of the structure are fixed to be solid or there is a finite minimum thickness of the structure like a fixed shell thickness in the reinforcement optimization of an engine hood. Alternatively, non-structural masses may be added to parts of the design domain.

Lecture 24: Summary



Top: A reinforcement problem. Maximization of the fundamental eigenvalue of a 5-bay tower structure where the outer frame structure is fixed to be solid.

Below: Maximization of the fundamental eigenvalue of a structure with nonstructural masses (each with a mass of 10% of the distributable mass) attached on the rightmost corners. The structures are shown in their fundamental mode of vibrations.

Lecture 24: Summary

Application: Forced vibrations

In some situations one may want to minimize or maximize the dynamical response of a structure for a given driving frequency or frequency range. An example of the former could be for an airplane where the vibrations in the structure should be minimized at the frequency of the propeller. For the latter, examples are a sensor which should give a large output for a certain driving frequency or a clock frequency generator that should vibrate at a certain frequency for least possible input.

For solving this type of design problem we define the dynamic compliance as driving force times magnitude of the displacement and express the goal for the dynamical response in terms of this compliance. An optimization problem solving the problem of minimizing the dynamic compliance of a structure subject to periodic forces, $\mathbf{f}(\Omega)$, with frequency Ω , can then be written as

$$\begin{aligned} \min_{\rho} \quad & \{ c = (\mathbf{f}^T \mathbf{u})^2 \} \\ \text{s.t. :} \quad & (\mathbf{K} - \Omega^2 \mathbf{M}) \mathbf{u} = \mathbf{f}, \\ & \sum_{e=1}^N v_e \rho_e \leq V, \quad 0 < \rho_{min} \leq \rho_e \leq 1, \quad e = 1, \dots, N. \end{aligned}$$

Lecture 24: Summary

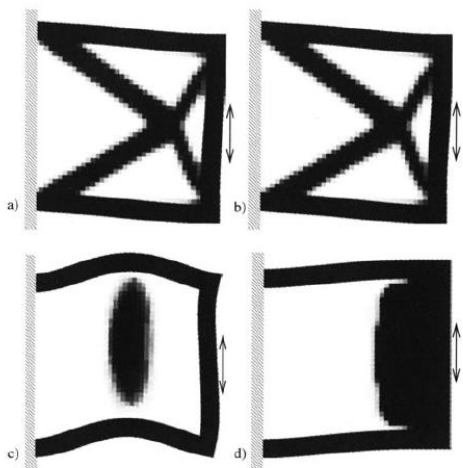
The sensitivities of the objective function may by use of the adjoint method be found as

$$\frac{\partial c}{\partial \rho_e} = \boldsymbol{\lambda}^T \left[\frac{\partial \mathbf{K}}{\partial \rho_e} - \Omega^2 \frac{\partial \mathbf{M}}{\partial \rho_e} \right] \mathbf{u},$$

where $\boldsymbol{\lambda}$ is the solution to the adjoint problem

$$(\mathbf{K} - \Omega^2 \mathbf{M}) \boldsymbol{\lambda} = -2(\mathbf{f}^T \mathbf{u}) \mathbf{f}.$$

We readily see from above that for low driving frequencies Ω , the results obtained should correspond roughly to the results of solving static problems (the term $\Omega^2 \mathbf{M}$ is a small perturbation to the stiffness matrix). However, for higher driving frequencies we should expect different resulting topologies. It can be shown that this formulation corresponds to forcing the closest eigenfrequency away from the driving frequency.



Optimized topologies for different driving frequencies . a) A zero driving frequency gives a statically stiff structure. b) while a small driving frequency forces the first eigenfrequency upwards resulting in a statically stiff structure. c) A larger driving frequency results in a tuned mass damper, d) and an even larger driving frequency forces the first eigenfrequency downwards and away from the driving frequency. All four examples were solved as reinforcement problems for a given outer frame and a stiffness ratio between black and white areas of 100:1. The structures are shown in their deformed states corresponding to the forced vibration mode.

Lecture 24: Summary

Application: Stress concentration

A stress criterion for the SIMP model

For the 0-1 formulation of the topology design problem a stress constraint is well-defined, but when a material of intermediate density is introduced, the form of the stress constraint is not a priori given.

A stress criterion for the SIMP model should be as simple as possible (like for the stiffness-density relation), and the isotropy of the stiffness properties should be extended to the stress model. Moreover, for physical relevance, it is reasonable that the criterion should mimic consistent microstructural considerations. This leads one to apply a stress constraint for the SIMP model (with exponent p) that is expressed as a constraint of the von Mises equivalent stress

$$\sigma_{\text{VM}} \leq \rho^p \sigma_l \quad \text{if } \rho > 0$$

Lecture 24: Summary

This constraint reflects the strength attenuation of a porous medium that arises when an average stress is distributed in the local microstructure, meaning that "local" stresses remain finite and non zero at zero density. This results in a reduction of strength domain by the factor ρ^p . We see that the same exponents are used for the stiffness interpolation and the stress constraint. Choosing another exponent is not consistent with physics and using an exponent that is less than p can for example lead to an artificial removal of material.

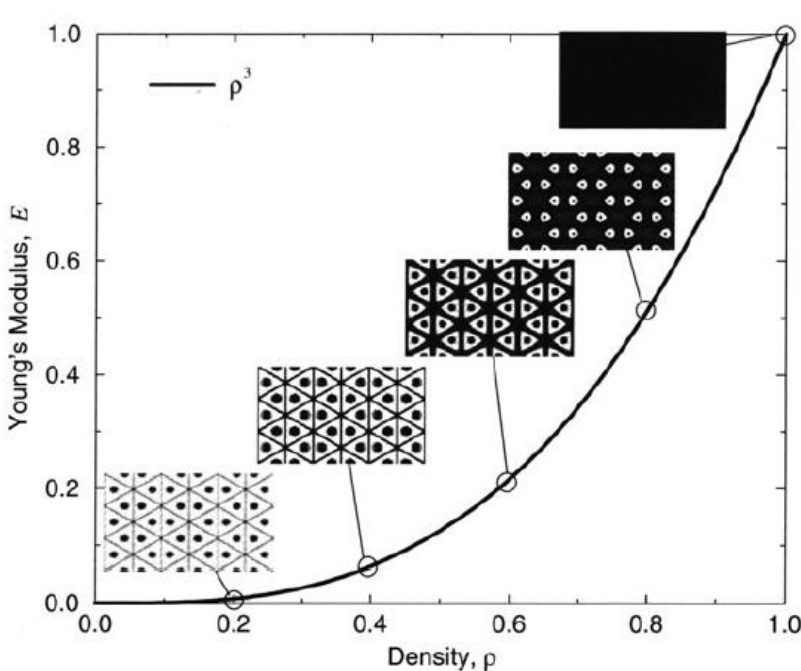
The classical stress-constrained optimization problem consists of finding the minimum weight structure that satisfies the stress constraint and which is in elastic equilibrium with the external forces, that is, we have a design problem in the form

$$\begin{aligned} \min_{\rho} \quad & \sum_{e=1}^N v_e \rho_e \\ \text{s.t. : } & \mathbf{Ku} = \mathbf{f}, \\ & (\sigma_e)_{VM} \leq \rho_e^p \sigma_l \text{ if } \rho > 0, \quad 0 < \rho_{min} \leq \rho_e \leq 1, \quad e = 1, \dots, N \end{aligned}$$

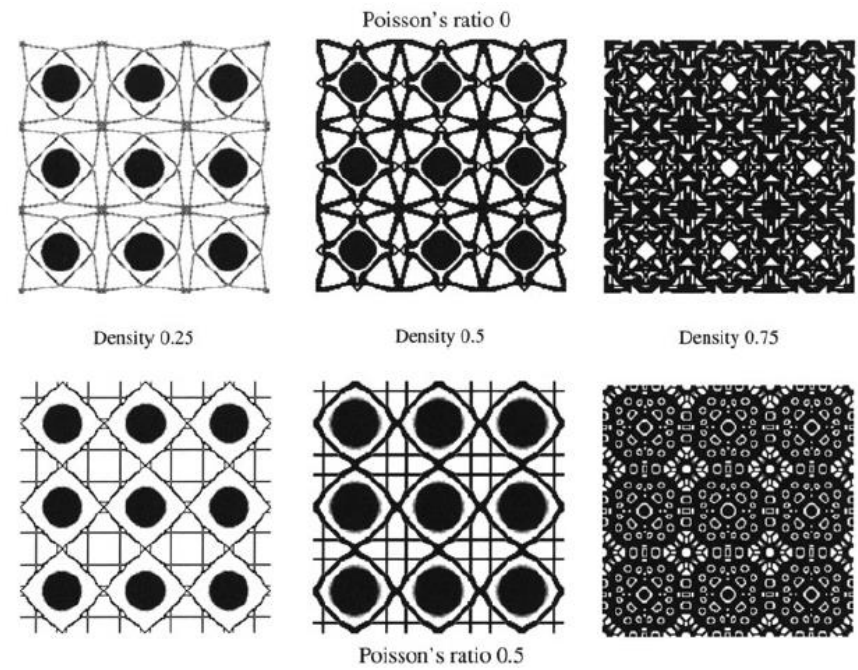
where the stress for example is evaluated at the center-node of the individual FE elements.

Lecture 24: Summary

A realization of the SIMP model We have continually compared the SIMP and other interpolation models with the Hashin-Shtrikman bounds for isotropic composites. These bounds give *necessary* conditions for the interpolation models. However, it is the material design methodology of the inverse homogenization method that allows us to construct concrete realizations of the SIMP model, as seen below. Note that, in itself, the inverse homogenization is based on a SIMP interpolation in the unit cell, making the dog bite its tail.



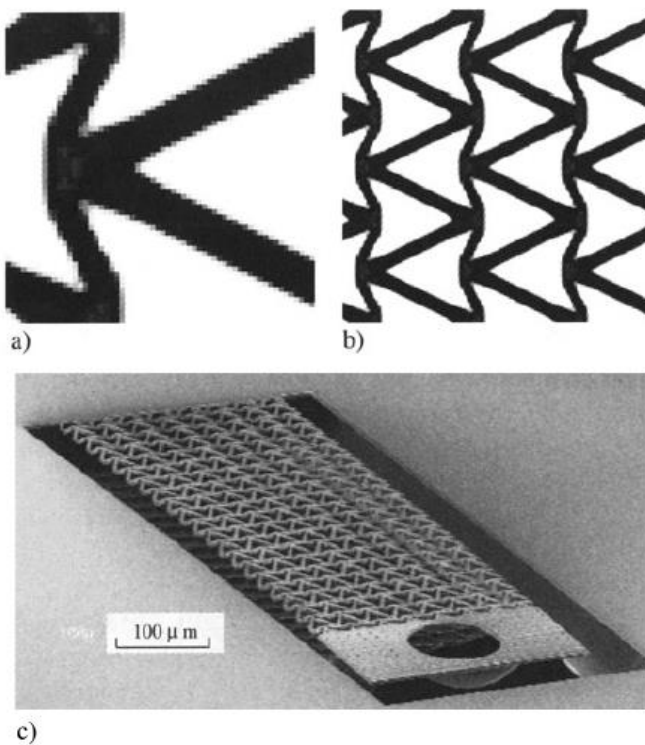
Microstructures of material and void realizing the material properties of the SIMP model with $p = 3$, for a base material with Poisson's ratio $\nu = 1/3$. As stiffer material microstructures can be constructed from the given densities, non-structural areas are seen at the cell centers



Microstructures of material and void realizing the material properties of the SIMP model with $p = 4$ for a base material with Poisson's ratio $\nu = 0$ (top row) and $\nu = 0.5$ (bottom row), respectively. As left figure, non-structural areas are seen at the centers of the cells

Lecture 24: Summary

Negative Poisson's ratio materials An extremely interesting application of the material design method is the search for negative Poisson's ratio materials. A number of such structures have been suggested in the literature, but here we apply topology optimization to obtain the behaviour we are looking for. If previous equation is formulated so as to minimize the Poisson's ratio with a constraint on bulk modulus and isotropy, the inverse homogenization method gives results as shown for 2D below.



The isotropic and negative Poisson's ratio structure has been manufactured in micro-scale. The 40 by 8 cell test beam was built using surface micromachining with a unit-cell size of $60 \mu\text{m}$ as shown in (c). The Poisson's ratio of the test-beam was measured to -0.9 ± 0.1 in experiments; this compares favourably to the theoretical value of -0.8.

Material microstructure with negative Poisson's ratio. a) one unit cell discretized by 60 by 60 elements, b) repeated unit cell and c) micromachined test beam built at MIC, DTU, DK

Lecture 24: Summary

Design with anisotropic materials

Layered material We now consider a layered material (cf., scale 2 of Fig. 3.2 rotated 90°) with layers directed along the y_2 -direction and repeated periodically along the y_1 -axis. The unit cell is $[0, 1] \times \mathbf{R}$, and it is clear that the unit cell fields χ^{kl} are independent of the variable y_2 . Also note that in Equation (3.2), the term involving the cell deformation field χ^{kl} is of the form $E_{ijpq}(x, y) \frac{\partial \chi_p^{kl}}{\partial y_q}$, so an explicit expression for χ^{kl} is not needed. Using periodicity and appropriate test functions and assuming that the direction of the layering coalesces with the directions of orthotropy of the materials involved, the only non-zero elements E_{1111} , E_{2222} , $E_{1212} (= E_{1221} = E_{2121} = E_{2112})$, $E_{1122} (= E_{2211})$ of the tensor E_{ijkl} can be calculated as shown in Appendix 5.4. Specifically, for a layering of two isotropic materials with the same Poisson ratio ν , with different Young's moduli E^+ and E^- and with layer thicknesses γ and $(1 - \gamma)$, respectively, the layering formulas (in plane stress) reduce to the following simple expressions:

$$E_{1111}^H = I_1, \quad E_{2222}^H = I_2 + \nu^2 I_1, \quad E_{1212}^H = \frac{1 - \nu}{2} I_1, \quad E_{1122}^H = \nu I_1, \\ I_1 = \frac{1}{1 - \nu^2} \frac{E^+ E^-}{\gamma E^- + (1 - \gamma) E^+}, \quad I_2 = \gamma E^+ + (1 - \gamma) E^-.$$

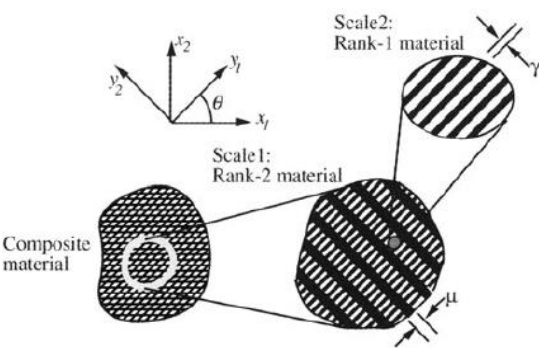


Figure 3.2

Lecture 24: Summary

It has been noted earlier that layered materials (so-called rank-N layered materials) play an important role as a class of composites for use in the homogenization approach. Such materials are created by successive layering of one material with composites already constructed. For example, the construction of a rank-2 layering is as follows. First, a (first order) layering of the strong and the weak material (void in the following) is constructed (see scale 2 of Fig. 3.2). This resulting composite material is then used as one of two components in a new layered material, with layers of the isotropic, strong material and of the composite just constructed; the layers of this composite material are placed at an angle to the direction of the new layering. The effective material properties of the resulting material can be computed by recursive use of the effective material parameters for a layering and the moduli are computed as the material is constructed, bottom up. The rank-N construction is analogous, and just includes more steps. For a rank-2 layering of material and void, with *perpendicular* layerings and with primary layerings of density μ in the 2-direction and the secondary layer of density γ in direction 1 (as in Fig. 3.2), the resulting material properties are:

$$E_{1111}^H = \frac{\gamma E}{\mu\gamma(1 - \nu^2) + (1 - \mu)}, \quad E_{1122}^H = \mu\nu E_{1111}^H,$$
$$E_{2222}^H = \mu E + \mu^2\nu^2 E_{1111}^H, \quad E_{1212}^H = 0,$$

Lecture 24: Summary

where E is Young's modulus and ν is Poisson's ratio of the base material. Also, the total density of the strong material in the unit cells of this rank-2 layered material is

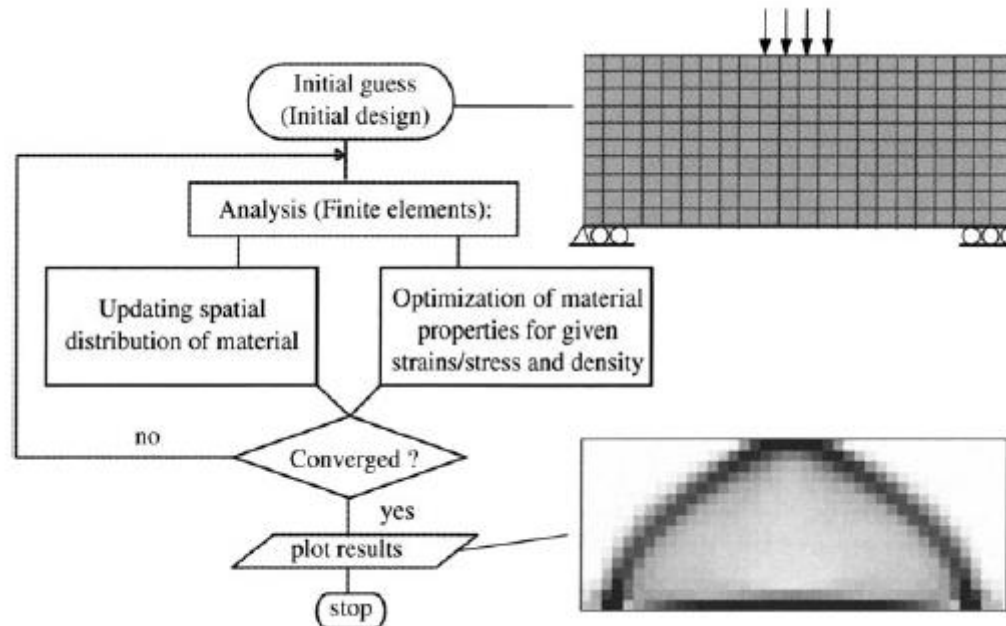
$$\rho = \mu + (1 - \mu)\gamma = \mu + \gamma - \mu\gamma .$$

The importance of the layered materials not only hinges on the analytical formulas for the effective material parameters. Of equal significance, studies on bounds on the effective material properties of composite mixtures made of two isotropic materials have shown that for elasticity the stiffest (or softest) material for a single load or multiple load problem can be obtained by a layered medium, with layering at several microscales. For single load problems the stiffest material consists of orthogonal layers, with no more than 2 layers for dimension 2 and no more than 3 layers for dimension 3. For multiple load problems the stiffest material (for the weighted average formulation) consists of layers that are not necessarily orthogonal, up to 3 for dimension 2 and up to 6 for dimension 3. The rank-2 materials are not the only composites which in 2-D achieves the upper bound on stiffness of a mixture of two materials. The layered materials are thus not special in the sense of being uniquely optimal, but they are special in the sense that their effective material properties can be expressed analytically.

Lecture 24: Summary

A hierarchical solution procedure

One of the advantages of the computational program just described is that the main flow of the procedure is *independent* of the modelling of the material used for the description of design. This latter information is added as an external module. This feature makes it possible to generate flexible procedures, where the material model can be changed easily.

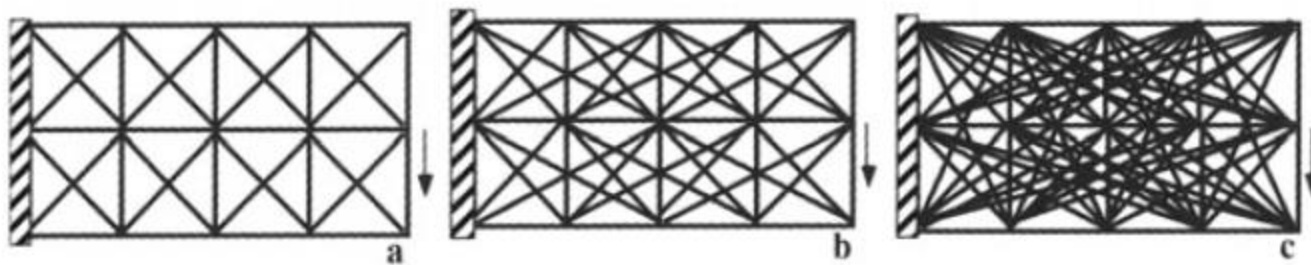


Optimal design using a hierarchical approach. The resulting structure is here a low volume solution to the problem

Lecture 24: Summary

Problem formulation for minimum compliance truss design

In the ground structure approach for truss topology design a set of n chosen nodal points (N degrees of freedom) and m possible connections are given, and one seeks to find the optimal substructure of this structural universe. In some papers on the ground structure approach, the ground structure is always assumed to be the set of all possible connections between the chosen nodal points, but here we allow the ground structure to be any given set of connections. This approach may lead to designs that are not the best ones for the chosen set of nodal points, but the approach implicitly allows for restrictions on the possible spectrum of possible member lengths as well as for the study of the optimal subset of members of a given truss-layout.



Ground structures for transmitting a vertical force to a vertical line of supports. Truss ground structures of variable complexity in a rectangular domain with a regular 5 by 3 nodal layout. In c) all the connections between the nodal points are included.

Lecture 24: Summary

Let a_i, l_i denote the cross-sectional area and length of bar number i , respectively, and we assume that all bars are made of linear elastic materials, with Young's moduli E_i . The volume of the truss is $V = \sum_{i=1}^m a_i l_i$. In order to simplify the notation at a later stage, we introduce the bar volumes $t_i = a_i l_i$, $i = 1, \dots, m$, as the fundamental design variables. Static equilibrium is expressed as

$$\mathbf{B}\mathbf{q} = \mathbf{f},$$

where \mathbf{q} is the member force vector and \mathbf{f} is the nodal force vector of the free degrees of freedom. The ground structure is chosen so that the compatibility matrix \mathbf{B} has full rank and so that $m \geq N$, excluding mechanisms and rigid body motions. The stiffness matrix of the truss is written as

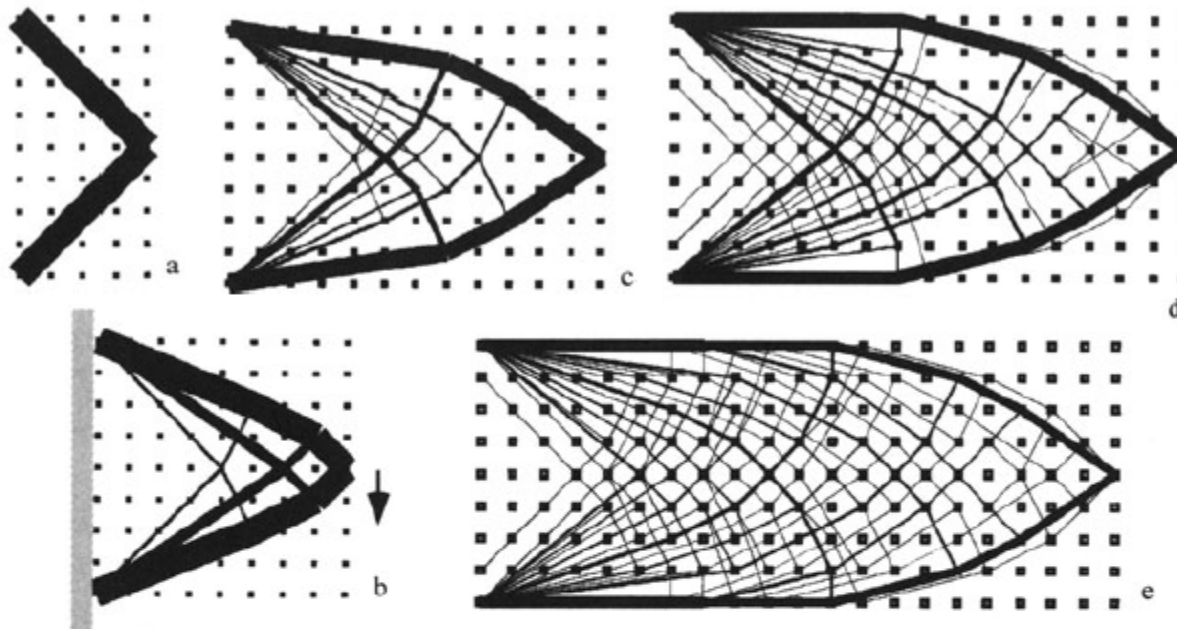
$$\mathbf{K}(\mathbf{t}) = \sum_{i=1}^m t_i \mathbf{K}_i,$$

where $t_i \mathbf{K}_i$ is the element stiffness matrix for bar number i , written in global coordinates. Note that $\mathbf{K}_i = \frac{E_i}{l_i^2} \mathbf{b}_i \mathbf{b}_i^T$ where \mathbf{b}_i is the i 'th column of \mathbf{B} .

The problem of finding the minimum compliance truss for a given volume of material (the stiffest truss) has the well-known formulation (cf., the continuum setting Sect. 1.1)

$$\begin{aligned} & \min_{\mathbf{u}, \mathbf{t}} \mathbf{f}^T \mathbf{u} \\ \text{s.t. : } & \sum_{i=1}^m t_i \mathbf{K}_i \mathbf{u} = \mathbf{f}, \quad \sum_{i=1}^m t_i = V, \quad t_i \geq 0, \quad i = 1, \dots, m. \end{aligned} \tag{4.1}$$

Lecture 24: Summary



The influence of the ground structure geometry on the optimal topology. Optimal truss topologies for transmitting a single vertical force to a vertical line of supports. The ground structures consist of all possible non-overlapping connections between the nodal points of a regular mesh in rectangles of varying aspect ratios $R = a/b$. a): 632 potential bars for 5 by 9 nodes in a rectangle with $R = 0.5$. Optimal non-dimensional compliance $\Phi = 4.000$. b): 2040 potential bars, 9 by 9 nodes, $R = 1.0$, $\Phi = 5.975$. c): 4216 potential bars, 13 by 9 nodes, $R = 1.5$, $\Phi = 9.1676$. d): 7180 potential bars, 17 by 9 nodes, $R = 2.0$, $\Phi = 12.5756$. e): 10940 potential bars, 21 by 9 nodes, $R = 2.5$, $\Phi = 16.4929$

Lecture 24: Summary

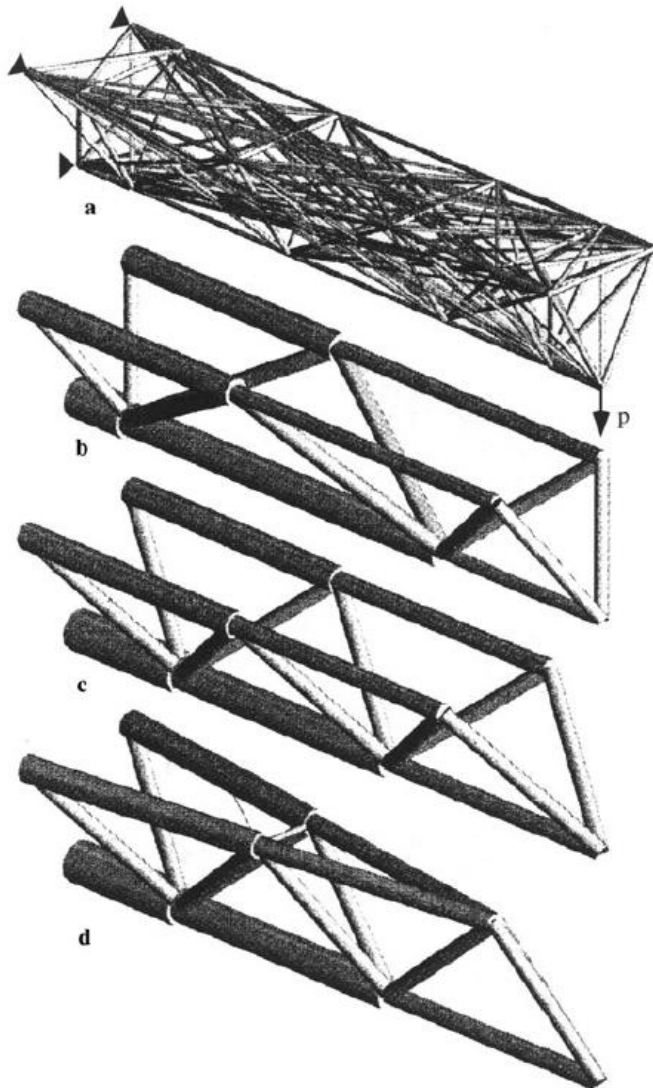
Extensions of truss topology design

1. Combined truss topology and geometry optimization

The topology design methods considered so far all employ the basic idea of a ground structure or reference design domain to obtain problem statements that are sizing problems for a fixed geometry. The choice of this reference geometry influences the result of the topology optimization making it important to consider sensitivity analysis of the optimal designs with respect to variation of the reference geometry, and even optimal design of this reference geometry may be fruitful in some situations.

In the ground structure approach to topology design of trusses the positions of nodal points are not used as design variables. This means that a high number of nodal points should be used in the ground structure to obtain efficient topologies. A drawback of the method is that the optimal topologies can be very sensitive to the layout of nodal points, at least if the number of nodal points is relatively low. This makes it natural to consider an extension of the ground structure approach and to include the optimization of the nodal point location for a given number and connectivity of nodal points. With very efficient tools at hand for the topology design with fixed nodal positions it seems natural to treat the variation of nodal positions as an outer optimization in a two-level hierarchical formulation. As the optimal value function of the topology compliance depends on the geometry variables in a non-smooth way, this outer minimization requires non-smooth optimization techniques.

Lecture 24: Summary

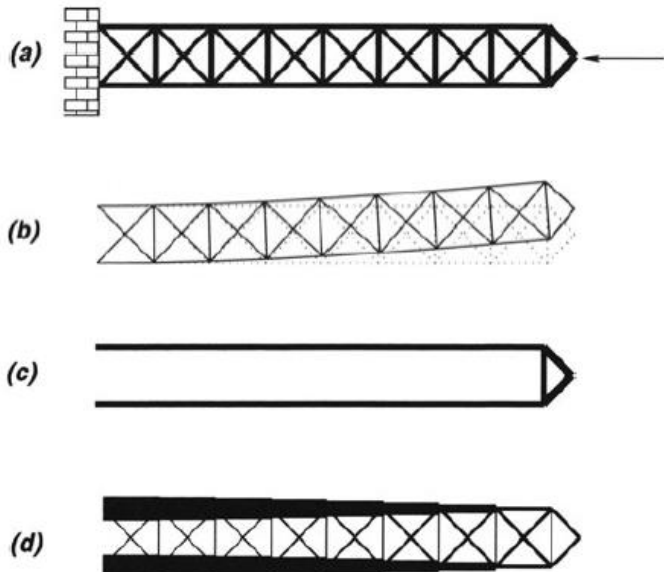


An example of a 3-D topology and geometry optimization for a beam carrying a single load. In a) we show the ground structure of nodal points and potential bars. Note that the ground structure has non-equidistant nodal point positions along the length axis of the "beam". In a) we see the optimal topology for the fixed nodal lay-out of the ground structure, in c) a combined geometry and topology optimization with nodal positions restricted to move along the length axis of the 'beam'. Finally, in d) the result of a combined geometry and topology optimization with totally free nodal positions is shown. The (non-dimensional) compliance values of the optimized designs are 1.00, 0.945 and 0.911, respectively.

Lecture 24: Summary

4.2 Truss design with buckling constraints

An example of what can be achieved with this formulation is illustrated in Figure below. Here the initial design has $t_i = 1000/m$, $i = 1, \dots, m$, with a corresponding compliance of 0.177 and a critical force (0.397) that is smaller than one, meaning that the truss is unstable. The standard truss optimization without stability constraint gives a design that is twice as light as the previous one but absolutely unstable. Finally, by truss optimization with stability constraint one can obtain a design that at a volume of 1179.6 is a bit heavier than the first one. However, it is stable under the given load. To see fully the effect of the stability constraint, we have for this example chosen the upper bound for the compliance so that the compliance constraint is not active. For truss (and frame) models *local* buckling of the individual members is also an important aspect to take into consideration.



The effect of a constraint on the global buckling load, a) shows the initial truss with its buckling mode in b). c) is the optimal truss without stability constraint and, d) is the optimal truss with a stability constraint.

Lecture 24: Summary

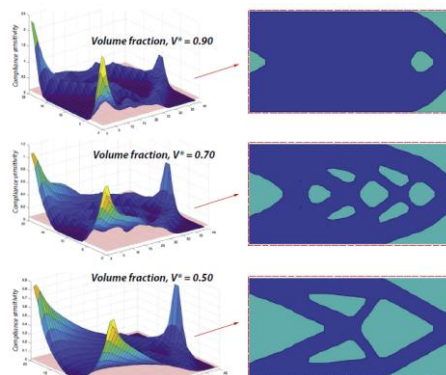
Topology optimization methods

The Michell truss

Ground structure

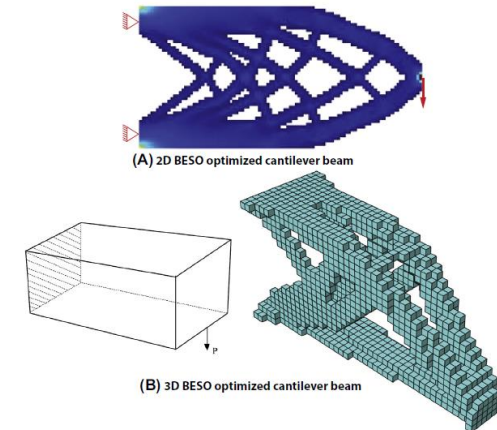
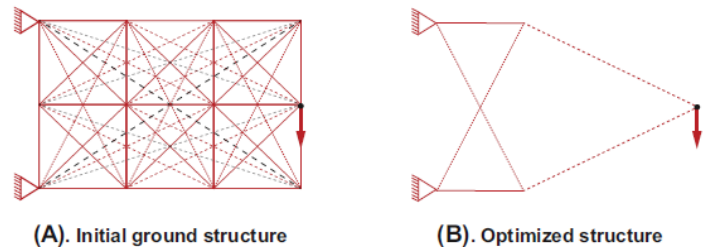
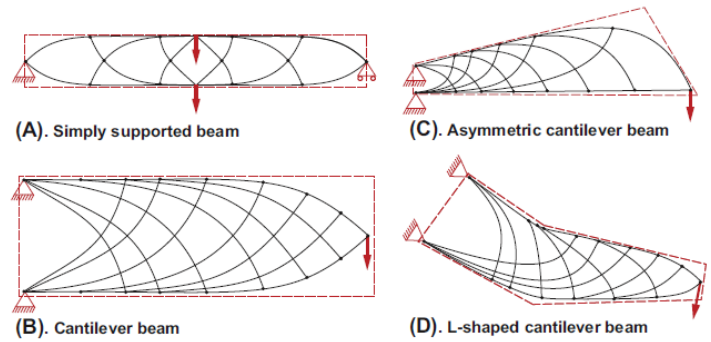
Level-set methods

Discrete (voxel) methods



Bidirectional evolutionary structural optimization (BESO) methods

Solid isotropic material with penalization (SIMP) method



Lecture 24: Summary

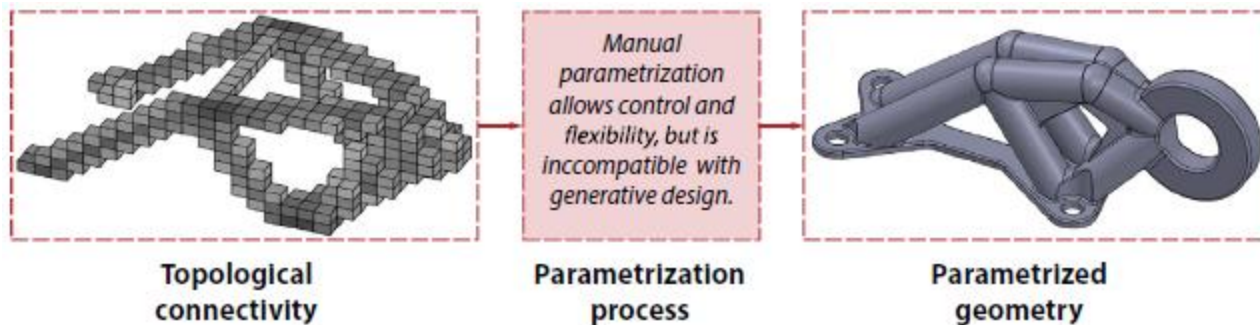
Parametric optimization

Brute force methods (DOE)

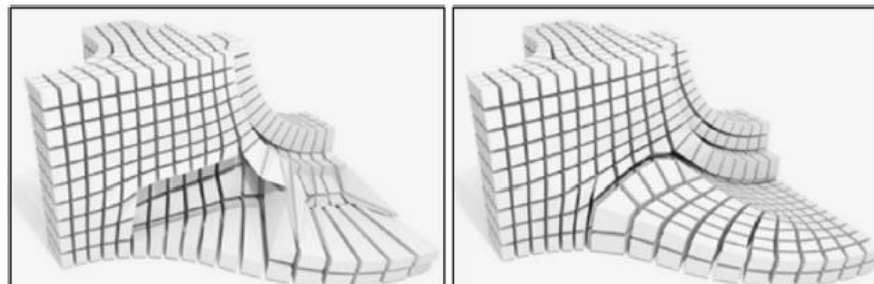
Sequential optimization methods: Gradient methods, Nelder-Meade simplex methods, etc

Topology optimization and generative design (BC2AM)

Automated extraction of parametric data from TO outcomes



Smoothed TO outcomes

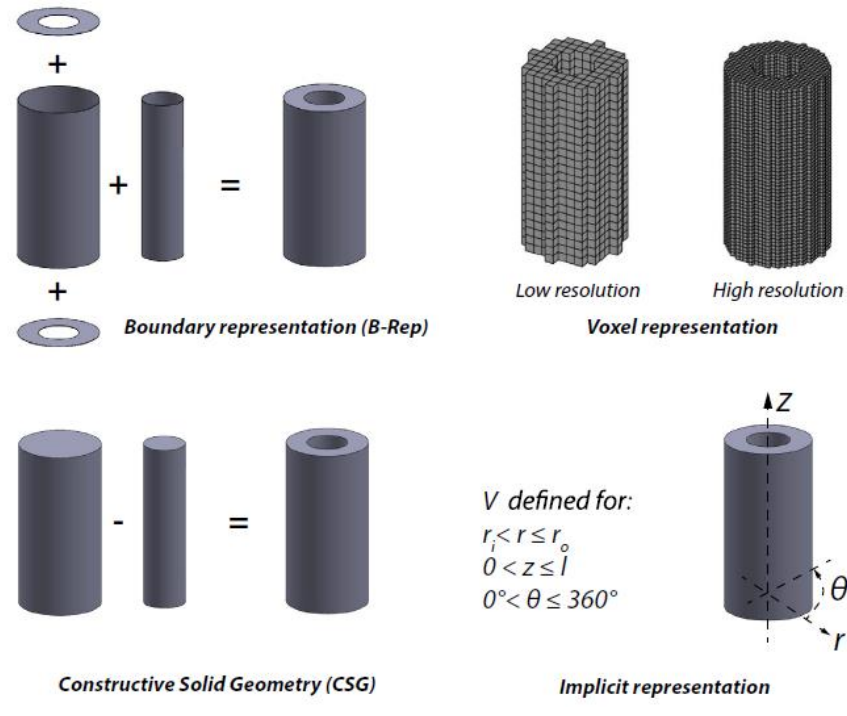


Lecture 24: Summary

Computer Aided Design (CAD)

Computer Aided Design (CAD) data provides unambiguous representations of the geometric envelope associated with a specific intended geometry. Numerous formal protocols for CAD representation exist and are defined for various purposes according to their specific capabilities and attributes. These attributes include the fundamental method of geometric representation, either as a volume or external surface; the representation of geometry as either explicit or implicit data; the associated data storage protocol; and the representation of either toleranced or nominal geometries.

CAD data can be generated according to numerous protocols. These protocols consist of both proprietary and open-source formats and can be classified according to the method of geometry generation. Prominent *explicit methods* for data generation include *Constructive Solid Geometry (CSG)* and *boundary representation (B-rep)*. *Implicit methods* for geometry representation include *voxel methods*, *level sets*, and *scalar fields* that indirectly represent the geometry of interest. Each of these methods has distinct opportunities and challenges for AM application.

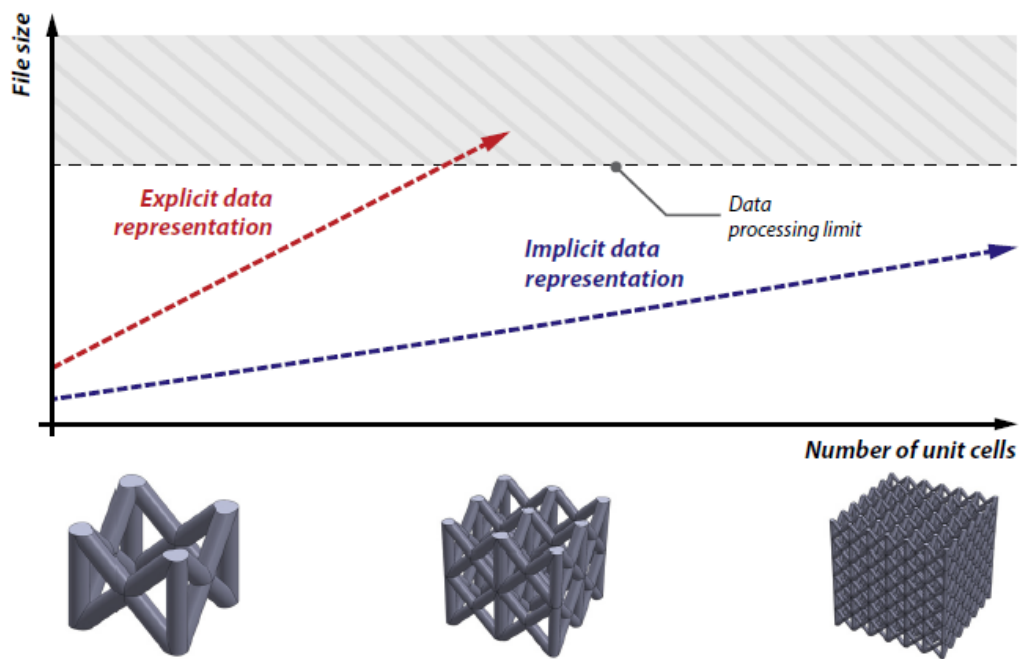


Lecture 24: Summary

Constructive Solid Geometry (CSG) represents the intended component geometry with Boolean operations applied to primitive geometry structures, such as spheres, cylinders and cubes. These CSG methods are therefore eminently compatible with algorithmic methods, as are required for generative AM design. However, these representations are not necessarily compatible with curvilinear geometries, which are not readily constructed from the available library of primitive structures.

Boundary representations (B-rep) consist of surface elements that interconnect to define the volume of interest. B-rep is robust and flexible, especially for curvilinear geometries including complex variable radius fillets and sweeping blends. Consequently, B-rep is often the preferred data representation used in manual CAD software. The explicit data representation of B-rep and CSG methods can be data-inefficient for repetitive geometries, including for self-tessellated lattice structures and the complex geometry that is often preferred for high-value AM applications. For these scenarios, the necessary file size can rapidly expand beyond the feasible data processing limit.

Schematic representation of explicit and implicit data representation of lattice structure. Data generated by commercially available tools with no data compression for repetition elements.

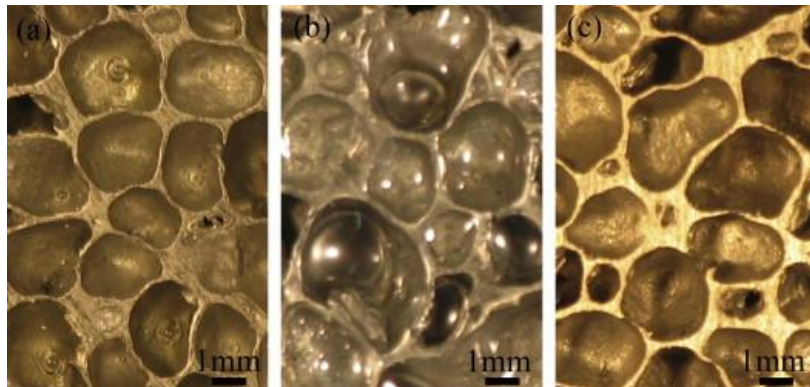


Lecture 24: Summary

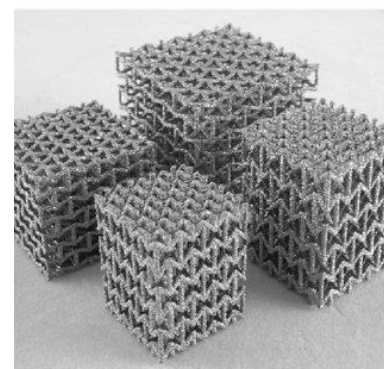
Classification of Cellular Materials



Random



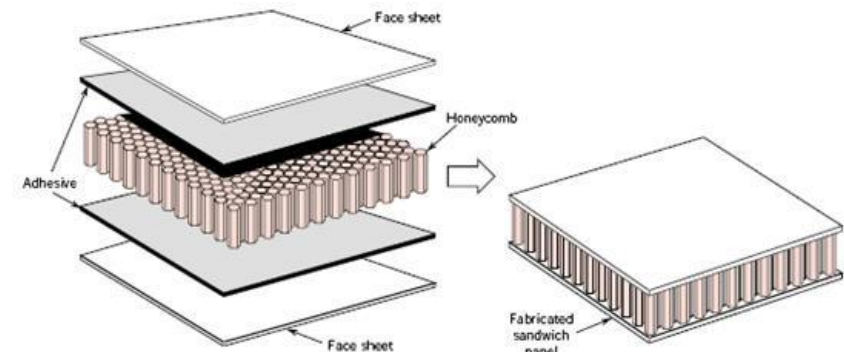
Open (pore)



Regular



Close

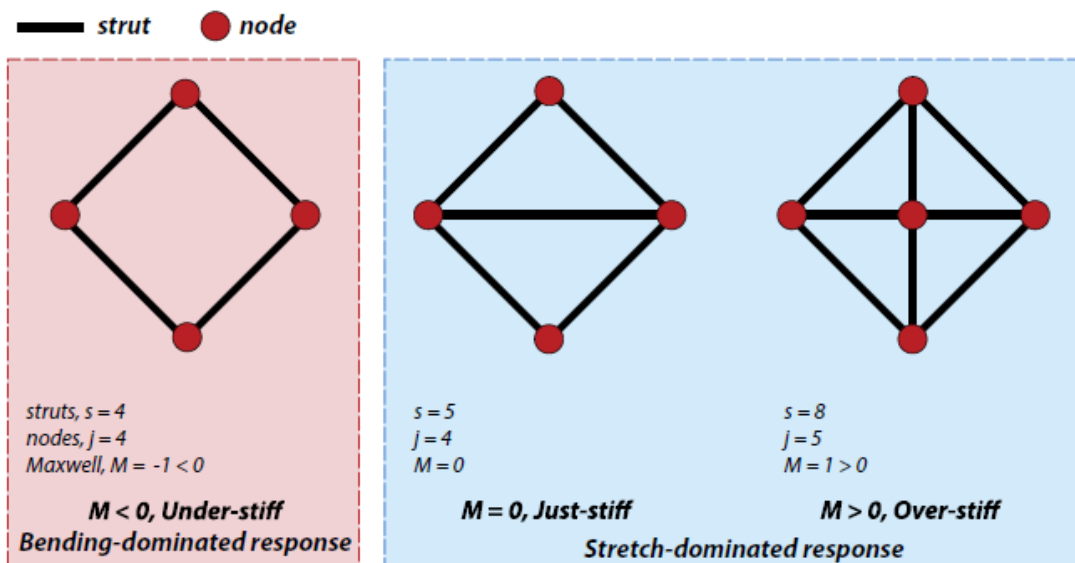


Lecture 24: Summary

Lattice structures

Lattice structures refer to the open-celled arrangement of strut elements with defined connectivity at specified nodes. These lattice arrangements are readily tessellated to fill space and allow highly efficient paths for the grounding of external and internal loads. Consequently, lattice structures are often observed in both naturally occurring biological systems such as the cellular structures of trabecular bone, and in engineered structural systems, for example three-dimensional truss structures used to efficiently ground loads in civil engineering structures. Lattice structures may have either stochastic or periodic arrangements. Biological lattice systems generally feature stochastic arrangements, whereas engineered lattice structures are typically periodic; however engineered structures with stochastic and hierarchical attributes are emerging within the research literature and in commercial applications.

Schematic representation of potential planar lattice configurations, Maxwell number, M and associated response type, either bending or stretch-dominated



Lecture 24: Summary

Maxwell stability criterion

Triangulated truss structures (known as space-frames in 3D space) provide a fundamentally efficient structural system. Such truss structures are typically designed to ground internal and external loads by a combination of tensile and compressive axial loading within the associated strut elements. For external loads to be robustly equilibrated by internal forces within the truss structure, a sufficient number of strut elements with appropriate nodal connectivity must exist. Maxwell proposed a set of mathematical conditions that must be satisfied for the loads be grounded in a mechanically robust manner. The Maxwell stability criterion is stated such that there are 2 free equilibrium-equations (3 for 3D space) associated with each node, j , and that each strut, s , represents an unknown equilibrating force; furthermore, there are 3 external forces (6 for 3D space), resulting in the inequalities

$$M = s - 2j + 3, \text{ for planar (2D) truss systems}$$

$$M = s - 3j + 6, \text{ for 3D space-frames}$$

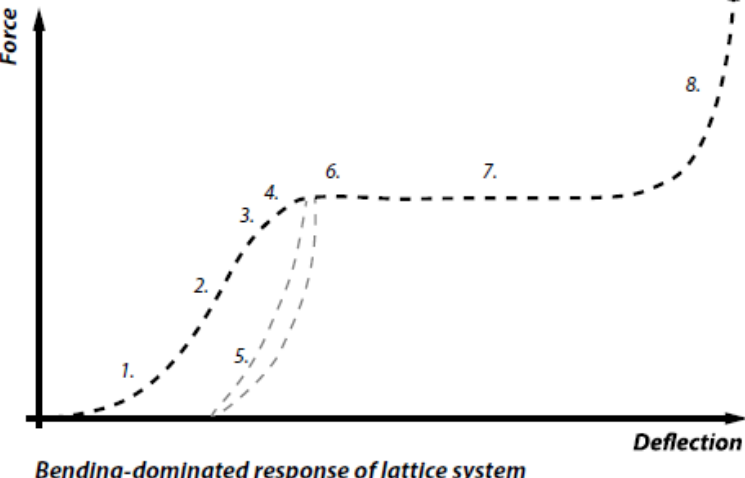
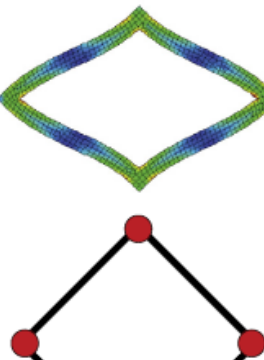
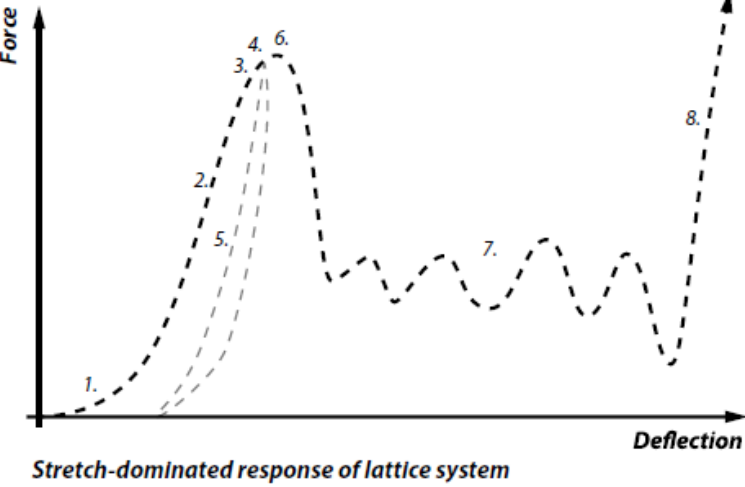
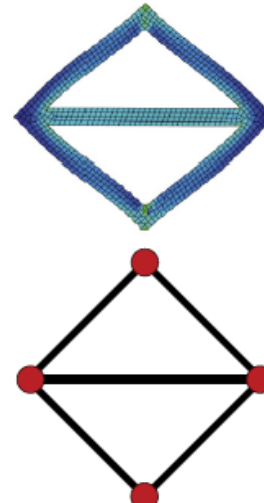
For scenarios where $M < 0$, there are insufficient struts to equilibrate the external forces, and the under-stiff truss system becomes a mechanism. For $M = 0$, the strut elements are arranged such that the strut loading is determinant for any external loading; such structures are defined as just-stiff and contain no structurally redundant strut elements. Additional strut elements can further increase the Maxwell number, $M > 0$, making the truss over-stiff.

Lecture 24: Summary

Observed mechanical response (lattice system)

Lattice system typically consists of an assemblage of individual unit cells. The mechanical response of such a lattice system is dependent on the structural response according to the Maxwell stability criterion. The overall behaviour of AM lattice systems has been documented both experimentally and mechanistically and may involve the following observed responses:

1. Initial plastic consolidation
2. Linear elastic response
3. Non-linear elastic response
4. Yield strength, or elastic limit
5. Unloading Modulus
6. Ultimate compressive strength
7. Crushing strength
8. Densification



Lecture 24: Summary

Prediction of AM lattice response

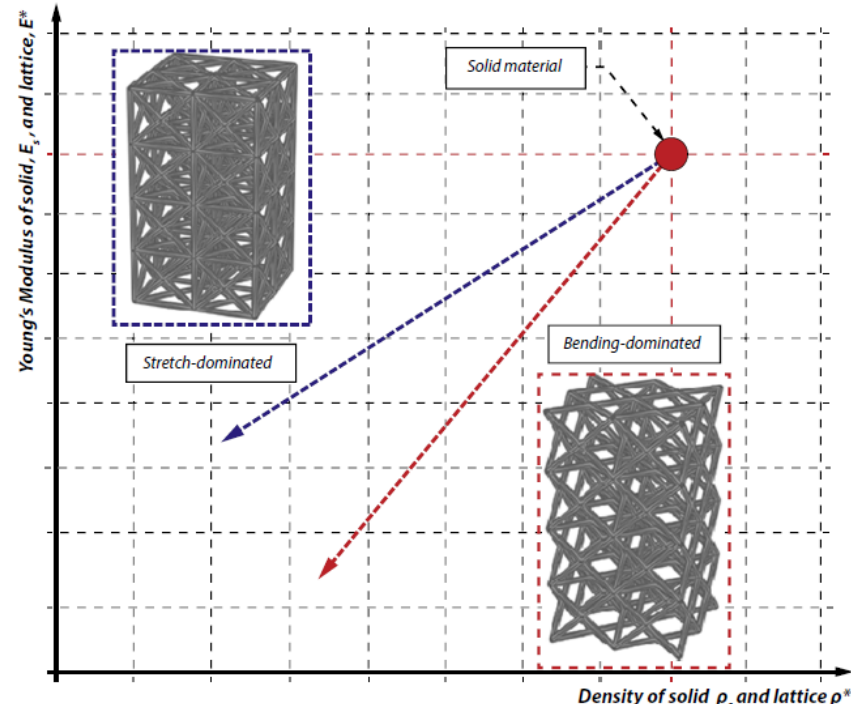
Numerous predictive models have been established to relate the lattice topology and material properties to the observed mechanical properties, most notably the seminal Gibson-Ashby model. This fundamental model is derived from first principles based on insights into cellular geometry and associated mechanical failure modes, resulting in predictive relationships of the type defined below. Specifically, these relationships predict the lattice mechanical response, P , to be proportional to some known response of the solid material P_s , and the ratio of lattice to solid material density, ρ^*/ρ_s , to the power of some exponent, n , and scaled by some proportionality constant, C . The predicted exponent depends on whether the structure is bending- or stretch-dominated as summarized in next Table for a number of pertinent scenarios.

$$P^* = C P_S \left(\frac{\rho^*}{\rho_S} \right)^n$$

Lecture 24: Summary

Response type	Mechanical property	Relationship
Bending-dominated	Modulus (E^*)	$E^* = CE_s \left(\frac{\rho^*}{\rho_s} \right)^2$
	Plastic collapse (σ_{pl}^*)	$\sigma_{pl}^* = C \sigma_{y,s} \left(\frac{\rho^*}{\rho_s} \right)^{1.5}$
	Elastic collapse (σ_{el}^*)	$\sigma_{el}^* = CE_s \left(\frac{\rho^*}{\rho_s} \right)^2$
Stretch-dominated	Modulus (E^*)	$E^* = CE_s \left(\frac{\rho^*}{\rho_s} \right)^1$
	Plastic collapse (σ_{pl}^*)	$\sigma_{pl}^* = C \sigma_{y,s} \left(\frac{\rho^*}{\rho_s} \right)^1$
	Elastic collapse (σ_{el}^*)	$\sigma_{el}^* = CE_s \left(\frac{\rho^*}{\rho_s} \right)^2$

A selection of Gibson-Ashby relationships for bending-dominated and stretch-dominated mechanical response.



Gibson-Ashby model illustrating Young's Modulus for bending and stretch-dominated structures with reference to the solid material.

Figure above provides further insight into the range of mechanical responses to be expected based on Gibson-Ashby relationships. Specifically, the Maxwell stability criterion can be used to directly characterize the lattice response as being either bending- or stretch-dominated. From this understanding, the Gibson-Ashby model can be utilized to predict the specific mechanical response of the associated lattice system. These predictions are compatible with the experimentally observed mechanical response of AM lattice structures; However, variability exists due to simplifications inherent in the Gibson-Ashby model and variation between the idealized and as manufactured AM lattice geometry. Due to the potential for variability in Gibson-Ashby model predictions, experimental results or validated numerical predictions are required for the design of high-value AM lattice applications.

Lecture 24: Summary

Post-processing for AM

All Additive manufacturing (AM) technologies require post-processing to produce parts that are ready for use. This post-processing can range from support material removal, to surface quality improvement, to colouring and painting, and to aging for polymer parts and heat-treatment for metal parts. Throughout the AM industry there is a vast amount of tacit knowledge in the area of post-processing but there, currently, exists very little documentation on the various post-processing methods for different AM technologies and materials. This leads to time being wasted by companies having to individually learn and develop post-processing methods. The overall process flow of additive manufacturing includes pre-processing and post-processing, and is presented in the following table. Note that the steps can vary, sometimes greatly, depending on the application, material, AM system being used, and specific requirements of the parts.



Metal powder-bed fusion	Polymer powder-bed fusion	Material extrusion	Vat photopolymerization	Binder jetting
Check quality of files and repair if necessary	Check quality of files and repair if necessary	Check quality of files and repair if necessary	Check quality of files and repair if necessary	Check quality of files and repair if necessary
Prepare print-job in software by arranging parts on build platform and generate support material	Prepare print-job in software by arranging parts on build platform	Prepare print-job in software by arranging parts on build platform and generate support material	Prepare print-job in software by arranging parts on build platform and generate support material	Prepare print-job in software by arranging parts on build platform
Clean AM system	Clean AM system	Clean AM system	Clean AM system	Clean AM system
Preheat build chamber	Preheat build chamber	Preheat build chamber		Preheat build chamber
Print	Print	Print	Print	Print
Remove build plate from build chamber	Find and remove parts from powder bed	Remove parts from build chamber	Drain and/or recycle unused material as applicable	Find and remove parts from powder bed
Remove loose powder and recycle	Recycle remaining powder	Remove support material	Remove parts from build chamber	Recycle remaining powder
Thermal stress relief	Media-blast parts to remove surface powder	Surface finish: sand, vapor smooth, paint, etc.	Remove support material	Air-blast parts to remove surface powder
Remove parts from build plate	Surface finish: tumble, sand, dye, paint, etc.	Inspect	Post-cure in UV chamber	Bake parts as necessary
Hot isostatic pressing	Inspect		Surface finish: sand, vapor smooth, paint, etc.	Strengthen with infiltration
Remove support structures			Inspect	Surface finish, sand, paint, etc.
Heat treat				Inspect
Surface machining, shot-peening, abrasive flow machining, etc.				
Inspect				

Thank you for your attention